Contrib Mineral Petrol (2000) 140: 84–98

Stephan Klemme · Hugh StC O'Neill

The effect of Cr on the solubility of Al in orthopyroxene: experiments and thermodynamic modelling

Received: 9 August 1999 / Accepted: 18 February 2000

Abstract The partitioning of chromium and aluminium between coexisting orthopyroxene and spinel in equilibrium with forsterite in the system $MgO–Al_2O_3–SiO_2–Cr_2O_3$ (MAS–Cr) has been experimentally determined as a function of temperature, pressure and Cr/(Cr + Al) ratio. Experiments were conducted at temperatures between 1300 and 1500 °C and at pressures from 5 to 54 kbar. Previous experimental results on the $(Al, Cr)_2O_3$ and $Mg(Al, Cr)_2O_4$ solid solutions have been combined with the present results plus relevant data from the CMAS system to derive a thermodynamic model for Al–Cr-bearing orthopyroxenes, spinels and corundum–eskolaite solid solutions. The orthopyroxene solid solution can be modelled within the accuracy of all experimental constraints as a ternary solid solution involving the components $Mg_2Si_2O_6$ (E), $MgAl_2SiO_6$ (M) and $MgCr_2SiO_6$ (C), in which the activities are related to composition through the equations:

$$RT\ln(a^{opx}_{Mg_2Si_2O_6}) = RT\ln(X^{opx}_E) + W^{opx}_{EM}(X^{opx}_E)^2 + W^{opx}_{EC}(X^{opx}_C)^2 + (W^{opx}_{EM} + W^{opx}_{EC} - W^{opx}_{MC})X^{opx}_M X^{opx}_C$$

$$RT\ln(a^{opx}_{MgAl_2SiO_6}) = RT\ln\left((X^{opx}_M)^2/(X^{opx}_M + X^{opx}_C)\right) + W^{opx}_{EM}(X^{opx}_E)^2 + W^{opx}_{MC}(X^{opx}_C)^2 + (W^{opx}_{EM} + W^{opx}_{MC} - W^{opx}_{EC})X^{opx}_E X^{opx}_C$$

$$RT\ln(a^{opx}_{MgCr_2SiO_6}) = RT\ln\left((X^{opx}_C)^2/(X^{opx}_M + X^{opx}_C)\right) + W^{opx}_{MC}(X^{opx}_M)^2 + W^{opx}_{EC}(X^{opx}_E)^2 + (W^{opx}_{MC} + W^{opx}_{EC} - W^{opx}_{EM})X^{opx}_M X^{opx}_E$$

The mole fractions are defined as

$$X^{opx}_E = (1 - n_{Al}/2 - n_{Cr}/2),\ X^{opx}_M = (n_{Al}/2) \text{ and } X^{opx}_C = (n_{Cr}/2),$$

where n_{Al} and n_{Cr} are the number of Al and Cr cations per orthopyroxene formula unit of six oxygens. These expressions reduce to one-site mixing for $Mg_2Si_2O_6$–$MgAl_2SiO_6$ orthopyroxenes in the Cr-free system, but are equivalent to two-site mixing for the exchange of Al and Cr between orthopyroxene and spinel, as required by the experimental data. We find $W^{opx}_{EM} = W^{opx}_{EC} =$ 20 kJ mol^{-1} and $W^{opx}_{MC} = 0$.

S. Klemme (✉)[1] · H. StC O'Neill
Research School of Earth Sciences, The Australian National University, Canberra, ACT 0200, Australia
e-mail: Stephan.Klemme@Bristol.ac.uk

Present address:
[1] Department of Earth Sciences,
Wills Memorial Building, Queen's Road, Bristol, BS8 1RJ, UK

Editorial responsibility: J. Hoefs

Introduction

More than 90% of the Earth's mantle is made up of the four oxide components CaO, MgO, Al_2O_3 and SiO_2 (e.g. O'Neill and Palme 1998), and therefore the simple system $CaO–MgO–Al_2O_3–SiO_2$ (CMAS) is often considered to make an excellent starting point for modelling mantle phase equilibria. However, many of the important details of mantle processes depend on the behaviour of the additional minor components, one of the most significant of which is Cr_2O_3.

Natural spinel lherzolites and garnet lherzolites contain on average about 2600 ppm chromium (O'Neill and Palme 1998). At typical terrestrial oxygen fugacities, nearly all of this chromium is in the trivalent oxidation state. Cr^{3+} is known to partition strongly among the major upper mantle phases, as illustrated by analyses of coexisting phases in a five-phase lherzolite xenolith (Table 1). The spinel in this example contains ~18 wt% Cr_2O_3, while the coexisting pyroxenes contain 0.5 and 1.2 wt% Cr_2O_3. However, because the pyroxenes are modally more abundant than the spinel, quite a large percentage of the bulk-rock chromium is contained in the pyroxenes. Clearly, an adequate thermodynamic model for Cr in mantle rocks requires knowledge of the properties of Cr-bearing pyroxenes.

An example of this need is provided by the recent work of Asimov et al. (1995) on melt productivity along the solidus of mantle peridotite. Their results indicated that melting may cease during adiabatic mantle upwelling as the boundary between garnet lherzolite and spinel

Table 1 Spinel–garnet lherzolite – Ming-Xi (China). Mineral analyses of a garnet–spinel-bearing lherzolite from China (Ming-Xi, province; Ai 1992) are depicted. Cr is concentrated in the spinel phase, which is abundant in only minor modal amounts. Modal amounts were calculated from bulk-rock analyses and mineral analyses (Ai 1992)

	Spinel	Garnet	Olivine	opx	cpx
MgO	20.1	20.7	49.1	32.8	15.9
Al_2O_3	49.9	23.1	–	4.6	6.0
Cr_2O_3	17.9	1.5	–	0.5	1.2
FeO	11.4	7.0	9.3	5.9	2.8
SiO_2	–	42.2	41.1	55.6	52.9
Modal	0.7	7.3	64.5	15.8	11.9

lherzolite is crossed. However, this result depends critically on the width of the garnet–spinel transition, which cannot at present be modelled accurately for lack of data on the partitioning of Cr into the pyroxenes.

In this study we investigate the effect of Cr on the solubility of Al in orthopyroxene in equilibrium with spinel and olivine in the system $MgO–Al_2O_3–SiO_2–Cr_2O_3$ (MAS–Cr) as a first step towards a better understanding of the influence of this element on upper mantle phase relations. A series of subsolidus experiments was conducted followed by thermodynamic analysis of the experimental results. These data were then combined with results in the system $CaO–MgO–Al_2O_3–SiO_2$ (CMAS) (Klemme 1998; Klemme and O'Neill 2000), to produce an internally consistent thermodynamic model that enables calculation of phase relations in Cr-bearing systems.

Thermodynamic background

The solubility of Al and Cr in orthopyroxene in equilibrium with olivine and spinel in the system MAS–Cr may be described by two equilibria:

$$\underset{\text{spinel}}{MgAl_2O_4} + \underset{\text{orthopyroxene}}{Mg_2Si_2O_6} = \underset{\text{orthopyroxene}}{MgAl_2SiO_6} + \underset{\text{olivine}}{Mg_2SiO_4} \quad (1)$$

$$\underset{\text{spinel}}{MgAl_2O_4} + \underset{\text{orthopyroxene}}{MgCr_2SiO_6} = \underset{\text{spinel}}{MgCr_2O_4} + \underset{\text{orthopyroxene}}{MgAl_2SiO_6} \quad (2)$$

Equilibrium (1) describes the solubility of alumina in orthopyroxene in equilibrium with spinel and olivine while equilibrium (2) describes the exchange of Al and Cr between coexisting spinel and orthopyroxene. Equilibrium (1) has been experimentally investigated in the systems $MgO–Al_2O_3–SiO_2$ (MAS) (e.g. Gasparik and Newton 1984), CMAS (e.g. Fujii 1977; Gasparik 1984; Sen 1985; Klemme 1998; Klemme and O'Neill 2000) and Na_2O–CMAS (NCMAS; Walter and Presnall 1994). The addition of CaO to the MAS system should have negligible effect on this reaction, since substitution of CaO into the phases partaking in the reaction is either minor (i.e. orthopyroxene, in which phase its effect tends to cancel out across the reaction since orthopyroxene components occur on both sides of the reaction), or negligible (in olivine and spinel). The addition of Na_2O to the system similarly has negligible effect.

Equilibrium (1) has been used as a geothermometer in the spinel lherzolite facies (e.g. Gasparik and Newton 1984; Witt-Eickschen and Seck 1991). However, the replacement of Al by Cr in orthopyroxene probably exerts a large influence, and this has not been allowed for in the calibrations of this equilibrium as a geothermometer.

From an experimental point of view, the effect of Cr on the Al content of orthopyroxene should be most obvious where the amount of Al in the orthopyroxene is greatest, which is at high temperatures, and in the spinel lherzolite facies, rather than in the garnet lherzolite facies. For example, the solubility of Al_2O_3 in orthopyroxene in the Cr-free system CMAS is about 8 wt% at 15 kbar and 1200 °C in equilibrium with spinel, but only about 1.5 wt% at 40 kbar at the same temperature, in equilibrium with garnet. Hence we have concentrated our experimental effort on reaction (1) rather than the possible alternative reaction:

$$\underset{\text{garnet}}{Mg_3Al_2Si_3O_{12}} = \underset{\text{orthopyroxene}}{MgAl_2SiO_6} + \underset{\text{orthopyroxene}}{Mg_2Si_2O_6} \quad (3)$$

that controls the solubility of alumina in orthopyroxene in equilibrium with garnet. However, the results of the present study should be applicable to garnet-bearing equilibria provided the thermodynamics of Cr-bearing garnets are sufficiently well understood.

Experimental and analytical techniques and procedures

All high-pressure, high-temperature experiments but one were performed in a conventional piston-cylinder apparatus (Boyd and England 1960) at temperatures from 1300 to 1500 °C and pressures between 0.5 and 4.0 GPa, using a 0.5-inch-diameter pressure assembly. The assembly consists of two inner parts of MgO (66% density) above and below the capsule, surrounded by three concentric shells: a graphite heater, a glass tube (Pyrex) and an outermost sleeve of NaCl, pressed to >95% of the theoretical density. Starting materials were sealed in platinum capsules, which were insulated from the graphite heater by a small Al_2O_3 sleeve, and separated from the thermocouple tip by a 0.5 mm Al_2O_3 disc. The sample was placed in the hot spot of the assembly, the location of which has been found in previous studies (W.O. Hibberson, personal communication).

Runs were performed using the "piston-out" routine. First, a pressure of ~2.5 kbar was applied. Then the sample was heated up to 550 °C to soften the glass. During the compression to the final run pressure, temperatures did generally not exceed 750 °C to prevent deformation of the graphite heater. The pressure was then raised to approximately 1 kbar higher than the final run value, and then lowered to run value when the final run temperature was achieved. Pressure was kept constant during runs to within ±0.2 kbar, by manual adjustment if necessary. In keeping with usual practice for piston-cylinder assemblies with NaCl sleeves, no correction for friction was applied (e.g. Johannes et al. 1971; Mirwald et al. 1975; Bose and Ganguly 1995). A check on the pressure calibration of our assembly, using the fayalite–ferrosilite–quartz univariant equilibrium at 1050 °C, was reported in Klemme and O'Neill (1997).

As regards friction corrections in piston-cylinder apparatus, Bose and Ganguly (1995) have shown that friction decays with time during an experiment. Moreover, these authors point out "Since the shear strength of the salts decreases with increasing temperature, the extent of friction correction should change with temper-

ature" (Bose and Ganguly 1995, p. 233). Bose and Ganguly (1995) also are of the opinion that friction may depend on the rate of compression or decompression. At higher pressures, bulging of the piston may become important, a source of friction quite unrelated to the nature of the pressure assembly used. Clearly the historical practice of applying a simple percentage correction to nominal pressures in piston-cylinder experiments is inappropriate. A more realistic approach to the friction problem is to use a low-friction pressure medium, such as NaCl, while also running for sufficient lengths of time that the friction decays. Bose and Ganguly (1995) have demonstrated decay of friction from 6.5% to zero in 30 h for their 0.5-inch cell, at temperatures far below those of this study. Consequently, because of the relatively long run times at high temperatures used in this study, we believe that possible errors in pressure due to friction are only very small. Finally we note that the phase relations addressed in this study are not sensitive to pressure, and that quite large errors in pressure would have little effect on the interpretation of our results.

The run at 5.4 GPa was performed in a piston-cylinder apparatus, which we have developed recently at the RSES to exploit newly available grades of tungsten carbide with high compressional strength. The pressure assembly was of similar design to those used in the conventional piston-cylinder runs, but with a CaF_2 outer sleeve, rather than NaCl. The length of the assemblage was tailored carefully to ensure that only a small length of the piston remained unsupported outside the pressure vessel after final compression. The run was initially compressed to a nominal pressure of 6.0 GPa. Decay of friction was then monitored by measuring the piston displacement using a transducer. Steady state conditions (i.e. both no further piston displacement, and no change in oil pressure to the piston), implying decay of most of the initial friction, was reached at 5.4 GPa after about 72 h.

To check whether Cr^{2+} was present in the experiments at sufficient concentrations to influence matters, a few runs were conducted with an internal Re–ReO_2 buffer to generate a high oxygen fugacity environment, approximately midway between the Ni–NiO and the Fe_3O_4–Fe_2O_3 buffers (Pownceby and O'Neill 1994b). The Re–ReO_2 buffer consisted of a fine-grained mixture of 50 mol% Re-metal with 50 mol% ReO_2. Neither Re nor ReO_2 reacted with the phases of interest in the experiments, hence the buffer mixture was mixed in with the starting materials. Results from the buffered runs were indistinguishable from unbuffered experiments, indicating no significant Cr^{2+} in the experiments. Another item of evidence against the presence of significant Cr^{2+} in all experiments is the lack of detectable Cr in olivine (detection limit ~600 ppm Cr with EDS and 150 ppm with WDS on the electron microprobe at RSES; Ware 1991).

Temperature measurement

Temperatures were measured with $Pt_{94}Rh_6$–$Pt_{70}Rh_{30}$ thermocouples (type B) inserted axially into the assembly inside two-bore high-purity Al_2O_3 tubing. Possible pressure effects on the emf of thermocouples were neglected. The temperature uncertainties are estimated to be less than ±15 °C in the temperature range of the present experiments.

Several thermocouples made from the same spools of wire as used in the piston-cylinder experiments were tested against the melting point of Au at atmospheric pressure, returning an apparent temperature of 1064 ± 1 °C, in good agreement with the recommended ITS-90 fixed point of 1064.2 °C (e.g. McGlashan 1990).

Type B thermocouples are much more resistant to the effects of contamination at high temperature than the more commonly used Pt–$Pt_{90}Rh_{10}$ (type S) or Pt–$Pt_{87}Rh_{13}$ (type R) thermocouples, under both oxidizing and reducing conditions (Metcalfe 1950; Walker et al. 1962; Brodowsky et al. 1998), although they are somewhat less sensitive. The reason for the superior performance under reducing conditions of type B thermocouples compared to those with a pure Pt leg is that the effect of impurities on the thermoelectric coefficient of Pt–Rh alloys is a markedly non-linear function of Pt/Rh composition. Therefore, a contaminating element such as Al or B produces a change in the thermoelectric coefficient of pure Pt relative to $Pt_{90}Rh_{10}$ or $Pt_{87}Rh_{13}$ which is considerably greater than the change of $Pt_{94}Rh_6$ relative to $Pt_{70}Rh_{30}$ (Brodowsky et al. 1998).

W–Re thermocouples have become increasingly popular for piston-cylinder experiments since Williams and Kennedy (1969) and Presnall et al. (1973) demonstrated their resistance to contamination in the piston-cylinder environment. Mao and Bell (1970), Mao et al. (1971), and Presnall et al. (1973) compared W–Re thermocouples with type S (Pt–$Pt_{90}Rh_{10}$) thermocouples, all finding that the W–Re thermocouples suffered less drift from contamination. It is important to note that even for the type S thermocouples, significant contamination effects (thermocouple drift) were only observed at 1600 °C or above, provided that the thermocouples were shielded by high-purity alumina, as used in this study. For example, Presnall et al. (1973) report drift rates of 1 °C h^{-1} at 1600 °C. Thus, we would not have expected significant drift by contamination in the experiments reported here even if we had used type S thermocouples, since our highest temperature experiments are at 1500 °C, for 24 h (cf. Presnall et al. 1973, their fig. 5). Type B thermocouples have not, to our knowledge, been similarly compared against W–Re thermocouples in the piston-cylinder apparatus. At ambient pressure in an argon atmosphere, Glawe and Szaniszlo (1972) found that the drift of type B thermocouples at 1327 °C was actually about half that of W–Re (or type S thermocouples).

Although they may be more resistant to contamination, W–Re thermocouples suffer from several disadvantages, the most serious of which is that their performance (i.e. emf vs. temperature characteristics) is often far different from the theoretical. We have tested several batches of $W_{97}Re_3$–$W_{75}Re_{25}$ plus one batch of $W_{95}Re_5$–$W_{74}Re_{26}$ thermocouple wire from various manufacturers over the last 4 years, by comparing them from 800 to 1400 °C directly against calibrated type S and type B thermocouples, at ambient pressure in a gas-mixing furnace, in argon and argon–10% hydrogen atmospheres. The W–Re thermocouples have been in error by up to 75 °C at 1400 °C, and no batch was closer to the theoretical calibration than 10 °C at 1400 °C. Moreover, thermocouples made from the same spools of wire have been found to differ by up to 15 °C at 1400 °C. From switching legs from the various batches of wire, we deduce that it is the thermoelectric coefficient of the $W_{97}Re_3$ leg which is primarily to blame. The $W_{97}Re_3$ wire is manufactured with additions of alumina and silica plus other oxide components that form an intergranular melt, to prevent recrystallization and grain growth, which would cause the wire to become unusably brittle. However, this process can result in large compositional inhomogeneities in the W/Re ratio of the wire on the scale of electron microprobe analysis. When a thermocouple is so far off its target performance, it is difficult to invest much trust in its behaviour.

As an additional test of the performance of type B thermocouples, a number of piston-cylinder experiments have been undertaken in our laboratory, at temperatures between 1350 and 1400 °C and various pressures, in which both type B and $W_{97}Re_3$–$W_{75}Re_{25}$ thermocouples were used simultaneously (Klemme and O'Neill 2000; U.H. Faul, personal communication, 1999). The thermocouples were inserted axially into the assembly as customary, using four-bore alumina. We find that after an initial change of the order of 10 °C during the first few hours, no drift of one thermocouple relative to the other is observable in runs lasting up to 400 h. The initial change we surmise is due to annealing of the $W_{97}Re_3$–$W_{75}Re_{25}$ wires (Burns and Hurst 1972); we note that Burns and Hurst (1972) recommend annealing of W–Re wires at 2400 K for 1 h in argon, a procedure admittedly not followed in our (or, we suspect most other) experimental petrology laboratories.

We have also found that the high-purity alumina used for the thermocouple insulator in our experiments is sufficiently strong to resist complete collapse even up to 10 kbar, resulting in significant oxidation of the W–Re wires in the vicinity of the steel plug at the top of the assembly. Lastly, type B thermocouples possess the convenient characteristic that, over the range 0 to 50 °C, their thermoelectric emf varies only between −2.5 and 2.5 μV, such that the temperature of the reference junction is unimportant.

In summary, we believe that type B thermocouples offer the best prospect of accurate temperature measurement in piston-cylinder experiments in the range 1300 to 1500 °C, the range of the present study. While W–Re thermocouples are clearly required at temperatures in excess of 1800 °C (i.e. near to and above the melting point of Pt-rich alloys), whether they are preferable to type B thermocouples in the intermediate range 1500 to 1800 °C requires further study.

The importance of the choice of thermocouple in the present experiments is that the reliability of the type B thermocouples permits long run times. For example, our run times of up to 400 h at 1300 °C are nearly an order of magnitude longer than the times used by Gasparik and Newton (1984) of 45.5 to 47 h at the same temperature in the Cr-free MAS system, and over two orders of magnitude longer than the times used by Perkins et al. (1981) of 1 to 3 h.

Starting materials

The starting mixtures (Table 2) consisted of mechanical mixes of synthetic crystalline materials, mostly $Mg(Cr,Al)_2O_4$ spinel solid solutions, $Mg_2Si_2O_6$ orthoenstatite and Mg_2SiO_4 forsterite. The starting mixture SM11, used for reversals, contained no forsterite.

Spinels were synthesized at 1500 °C at atmospheric pressure under flowing CO_2 which produces a slightly reduced environment to prevent any oxidation of Cr^{3+} to Cr^{4+}. $Mg_2Si_2O_6$ (clinoenstatite) was synthesized at 1100 °C at atmospheric pressure in air. This material transforms rapidly to orthoenstatite at high pressures. These synthesis experiments were carried out for ~24 h. Forsterite (Mg_2SiO_4) was synthesized from MgO and SiO_2 using a Li_2WO_4 flux, with a flux:oxide ratio of 4:1 by weight. The flux:oxide mixture was held for 6 days at 1050 °C in a Pt crucible, before cooling to room temperature and removing the flux by dissolution in warm water with the aid of ultrasonic agitation.

Most experiments approached equilibrium as regards orthopyroxene compositions from the Cr- and Al-poor side, since the orthopyroxene in the starting materials was pure $Mg_2Si_2O_6$. Equilibrium in such experiments is indicated if, firstly, a change in orthopyroxene compositions is observable (which is sufficient to clarify that diffusion rates are fast enough to cause change), and, secondly, if the final orthopyroxenes and also the other solid solution phases (here, spinel) are homogenous in composition. All experiments reported here fulfil these dual criteria. Two quasi-reversal experiments were also performed to further confirm the achievement of equilibrium. These experiments contained a mixture of two different starting pyroxenes (SM47), one with high Al_2O_3 and Cr_2O_3 content, the other the pure $Mg_2Si_2O_6$. Analyses of the run products indicated that both types of pyroxenes converge completely onto a single population in the run product. The high Al/Cr orthopyroxene in SM 47 was crystallized from a melt at 19 kbar in a 5/8-inch piston-cylinder apparatus. The synthesis was conducted by heating to 1700 °C for 5 min (to induce melting), then cooling at 2 °C/min to 1550 °C, at which temperature the run was held for 10 h. The sample was then cooled at a rate of 1 °C/min down to 1300 °C, resting at 1300 °C for 24 h before quenching.

Preliminary experiments established that the Cr partitioning reactions proceed sluggishly. To evaluate the run durations needed for attainment of equilibrium in the experiments, series of experiments were conducted with different run times. At 1400 °C run durations of >120 h were found to be necessary to produce homogenous mineral compositions (Table 3). Experiments at 1300 °C had to be run for several weeks, but even then the mineral analyses showed larger scatter than at higher temperatures (Table 4). Attempts at 1200 °C produced only inhomogeneous pyroxenes and are not reported.

Table 2 Starting materials. All starting material mixtures contained synthetic Mg_2SiO_4 as well as $Mg_2Si_2O_6$ with the exception of SM 11 (no Mg_2SiO_4). SM 47 contained two starting pyroxenes: pure enstatite as well as an orthopyroxene with ~10 wt% Al_2O_3 and 0.8 wt% Cr_2O_3. See text for details and notes on the synthesis of the starting materials

Mixture	Spinel	Buffer
SM 11	$Mg(Cr_{0.5}Al_{0.5})_2O_4$	–
SM 16	$Mg(Cr_{0.5}Al_{0.5})_2O_4$	–
SM 34	$Mg(Cr_{0.46}Al_{0.54})_2O_4$	–
SM 35	$Mg(Cr_{0.57}Al_{0.43})_2O_4$	–
SM 41	$Mg(Cr_{0.8}Al_{0.2})_2O_4$	–
SM 42	$Mg(Cr_{0.2}Al_{0.8})_2O_4$	–
SM 47	$Mg(Cr_{0.46}Al_{0.54})_2O_4$	$Re–ReO_2$
SM 50	$Mg(Cr_{0.9}Al_{0.1})_2O_4$	–
SM 53	$Mg(Cr_{0.1}Al_{0.9})_2O_4$	–

Analytical procedures

Experimental run products were cut into halves using a low-speed diamond saw and mounted in epoxy resin for electron microscopy and microprobe analysis. Mounts were polished in several steps using sandpaper and diamond paste of different grain sizes. The final polish was performed with 0.3 μm Linde B polishing powder.

Table 3 Experimental runs in the system $MgO–Al_2O_3–SiO_2–Cr_2O_3$. Experimental run conditions and starting material are listed for each experiment. See text for details. *P* Pressure (kbar), *T* temperature (°C), *t* run duration (h). *spl* spinel, *ol* olivine, *opx* orthopyroxene, *gar* garnet

Run no.	*P* (kbar)	*T* (°C)	*t* (h)	Starting material	Phases present
C 301-S 38	40	1300	244	11	spl, ol, opx
C 297-S 36	25	1300	260	11	spl, ol, opx
C 586-S 114 I	25	1300	360	41	spl, ol, opx
C 587-S 114-II	25	1300	360	42	spl, ol, opx
C 598-S 118-I	10	1300	400	42	spl, ol, opx
C 599-S 118-II	10	1300	400	41	spl, ol, opx
C 517-S101-I	10	1300	240	35	spl, ol, opx
UHP 28-S 126	54	1400	120	50	spl, ol, opx
C 543-S 104-I	40	1400	120	16	spl, ol, opx
C 544-S 104-II	40	1400	120	34	spl, ol, opx
C-545-S 104-III	40	1400	120	35	spl, ol, opx
C 299-S 37	35	1400	144	11	spl, ol, opx
C 576-S 111-I	35	1400	120	41	spl, ol, opx
C 577-S 111-II	35	1400	120	42	spl, ol, opx, gar
C 623-S 123-I	35	1400	120	47	spl, ol, opx
C 624-S 123-II	35	1400	120	50	spl, ol, opx
C 233-S 22	24	1400	24	11	spl, ol, opx
C 587-S 115-I	24	1400	120	42	spl, ol, opx
C 588-S 115-II	24	1400	120	41	spl, ol, opx
C 591-S 116-I	20	1400	150	41	spl, ol, opx
C 592-S 116-II	20	1400	150	42	spl, ol, opx
C 724-S 130	20	1400	120	53	spl, ol, opx
C 730-S 131	15	1400	120	53	spl, ol, opx
C 326-S 50	10	1400	120	16	spl, ol, opx
C 577-S 112-I	10	1400	120	42	spl, ol, opx
C 578-S 112-II	10	1400	120	41	spl, ol, opx
C 618-S 122-I	5	1400	120	41	spl, ol, opx
C 689-S 127-I	5	1400	122	50	spl, ol, opx
C 690-S 127-III	5	1400	122	47	spl, ol, opx
C 329-S 51	35	1500	24	11	spl, ol, opx
C 596-S 117-I	35	1500	24	42	spl, ol, opx, gar
C 597-S 117-II	35	1500	24	41	spl, ol, opx
C 323-S 47	25	1500	24	11	spl, ol, opx
C 578-S 113-I	25	1500	24	41	spl, ol, opx
C 579-S 113-II	25	1500	24	42	spl, ol, opx
C 685-S 124	15	1500	24	50	spl, ol, opx
C 325-S 49	10	1500	24	11	spl, ol, opx

Table 4 Analytical results. *Cr # (bulk)* is Cr/(Cr + Al) in starting material. *T* temperature in (°C). *P* pressure in (kbar). Numbers show average analyses for each phases, numbers in brackets indicate uncertainties. For example, 1.759(18) must be read as 1.759 ± 0.018. At least ten analyses were done for each phase in every experiment

P (kbar)	40		25		25		25	
T (°C)	1300		1300		1300		1300	
Cr # (bulk)	50		50		80		20	
	OPX S 38	SPI S 38	OPX S 36	SPI S 36	OPX S 114-I	SPI S 114-I	OPX S 114-II	SPI S 114-II
SiO_2	57.1(4)	0.4(2)	57.7(4)	0.5(4)	59.4(7)	0.4(2)	56.6(7)	0.6(1)
Al_2O_3	3.2(2)	28.1(6)	2.7(5)	28.0(7)	0.9(1)	10.2(8)	5.9(9)	53.0(14)
Cr_2O_3	1.9(1)	45.8(9)	1.6(2)	45.9(8)	1.4(1)	66.0(7)	1.2(3)	20.5(17)
MgO	37.6(2)	22.8(3)	38.0(3)	22.8(2)	39.1(6)	20.9(3)	37.2(5)	25.8(4)
Total[a]	99.8	97.1	100.0	97.2	100.8	97.5	100.9	99.9
Si	1.923(4)	0.012(5)	1.937(14)	0.013(12)	1.976(4)	0.013(5)	1.881(21)	0.014(2)
Al	0.128(7)	0.954(19)	0.106(21)	0.950(23)	0.037(5)	0.374(28)	0.232(37)	1.584(34)
Cr	0.051(1)	1.043(20)	0.043(6)	1.046(19)	0.037(2)	1.626(25)	0.032(7)	0.412(34)
Mg	1.885(4)	0.981(9)	1.902(14)	0.980(6)	1.938(5)	0.974(7)	1.842(24)	0.977(6)
Total	3.987(1)	2.990(3)	3.988(2)	2.989(3)	3.987(2)	2.987(2)	3.987(3)	2.987(3)

P (kbar)	10		10		10		54	
T (°C)	1300		1300		1300		1400	
Cr # (bulk)	20		80		57		90	
	OPX S 118-I	SPI S 118-I	OPX S 118-II	SPI S 118-II	OPX S101-I	SPI S101-I	OPX S 126	SPI S 126
SiO_2	57.2(10)	0.5(1)	59.6(7)	0.4(0)	58.3(6)	0.3(1)	59.3(6)	0.6(1)
Al_2O_3	4.3(10)	50.6(6)	0.7(2)	11.0(7)	1.3(4)	22.7(30)	0.8(2)	4.6(1)
Cr_2O_3	1.1(3)	21.4(7)	1.3(2)	64.6(5)	1.2(3)	50.5(28)	1.3(1)	72.1(6)
MgO	38.0(6)	25.5(2)	39.6(5)	20.7(7)	38.5(6)	21.9(5)	39.2(4)	20.4(4)
Total	100.6	98.0	101.2	96.7	99.3	95.4	100.6	97.7
Si	1.909(24)	0.013(1)	1.975(5)	0.012(2)	1.969(11)	0.010(2)	1.978(7)	0.020(2)
Al	0.168(40)	1.549(14)	0.027(7)	0.407(21)	0.053(16)	0.802(87)	0.040(8)	0.171(4)
Cr	0.028(7)	0.440(14)	0.035(6)	1.598(30)	0.032(7)	1.199(86)	0.035(4)	1.820(17)
Mg	1.887(27)	0.990(3)	1.957(13)	0.967(21)	1.936(16)	0.980(9)	1.947(13)	0.973(17)
Total	3.992(7)	2.992(1)	3.994(5)	2.985(7)	3.990(6)	2.990(3)	3.990(6)	2.984(5)

P (kbar)	40		40		40		35	
T (°C)	1400		1400		1400		1400	
Cr # (bulk)	50		46		57		50	
	OPX S 104-I	SPI S 104-I	OPX S 104-II	SPI S 104-II	OPX S 104-III	SPI S 104-III	OPX S 37	SPI S 37
SiO_2	57.1(11)	0.4(1)	55.7(4)	0.7(2)	56.6(7)	0.6(4)	56.7(15)	0.5(2)
Al_2O_3	4.6(4)	29.8(16)	4.9(2)	33.8(66)	3.8(2)	22.9(17)	3.9(1)	28.0(8)
Cr_2O_3	2.6(6)	47.2(16)	2.3(3)	39.8(70)	2.3(2)	52.4(18)	2.3(1)	47.0(11)
MgO	38.1(6)	23.9(2)	36.9(8)	23.9(10)	37.7(4)	22.3(6)	37.5(4)	23.2(3)
Total	102.4	101.3	99.8	98.2	100.4	98.2	100.4	98.7
Si	1.878(21)	0.012(4)	1.879(8)	0.019(5)	1.896(7)	0.018(10)	1.901(15)	0.014(5)
Al	0.180(15)	0.968(45)	0.193(6)	1.103(176)	0.151(7)	0.788(47)	0.154(8)	0.937(26)
Cr	0.068(15)	1.028(39)	0.063(8)	0.880(176)	0.061(4)	1.208(57)	0.061(2)	1.055(25)
Mg	1.871(6)	0.981(5)	1.859(19)	0.988(9)	1.890(9)	0.970(12)	1.876(20)	0.984(7)
Total	3.997(7)	2.989(2)	3.994(9)	2.990(3)	3.998(4)	2.984(6)	3.992(11)	2.990(2)

P (kbar)	35		35			35		35	
T (°C)	1400		1400			1400		1400	
Cr # (bulk)	80		20			46		90	
	OPX S 111-I	SPI S 111-I	OPX S 111-II	SPI S 111-II	GAR S 111-II	OPX S 123-I	SPI S 123-I	OPX S 123-II	SPI S 123-II
SiO_2	59.3(2)	0.5(0)	55.5(10)	0.6(1)	43.9(12)	55.9(7)	0.6(1)	59.7(6)	0.4(1)
Al_2O_3	1.0(1)	9.7(4)	6.6(7)	50.8(13)	23.1(5)	5.4(8)	32.1(7)	0.7(1)	5.6(3)
Cr_2O_3	1.5(3)	66.8(13)	1.5(3)	20.7(13)	4.0(8)	2.0(3)	42.2(6)	1.6(3)	72.8(25)
MgO	37.9(5)	20.4(4)	36.1(8)	24.9(4)	29.4(5)	38.7(56)	23.7(3)	39.8(5)	21.7(13)
Total	99.7	97.4	99.7	97.0	100.4	101.9	98.6	101.8	100.5
Si	1.992(11)	0.014(1)	1.867(18)	0.016(2)	2.973(75)	1.853(74)	0.015(2)	1.969(9)	0.013(3)
Al	0.041(3)	0.358(15)	0.262(27)	1.567(27)	1.842(33)	0.209(33)	1.057(15)	0.028(5)	0.203(16)
Cr	0.040(7)	1.655(19)	0.041(8)	0.429(27)	0.215(43)	0.052(8)	0.933(19)	0.042(8)	1.780(26)
Mg	1.895(15)	0.951(11)	1.812(33)	0.973(2)	2.968(66)	1.902(164)	0.985(8)	1.956(8)	1.001(34)
Total	3.968(8)	2.978(4)	3.982(12)	2.985(1)	7.998(47)	4.016(79)	2.990(3)	3.995(4)	2.997(12)

Table 4 (Contd.)

P (kbar)	24		24		24		20	
T (°C)	1400		1400		1400		1400	
Cr # (bulk)	50		20		80		80	
	OPX	SPI	OPX	SPI	OPX	SPI	OPX	SPI
	S 22	S 22	S 115-I	S 115-I	S 115-II	S 115-II	S 116-I	S 116-I
SiO_2	58.0(8)	0.7(3)	56.0(8)	0.7(1)	59.9(5)	0.4(1)	59.0(3)	0.4(0)
Al_2O_3	3.2(7)	28.0(3)	6.5(10)	51.8(15)	0.9(2)	9.4(4)	1.1(2)	10.1(2)
Cr_2O_3	2.0(3)	46.4(3)	1.6(3)	20.9(18)	1.5(2)	67.7(9)	1.6(2)	65.7(1)
MgO	37.9(4)	23.2(3)	36.5(4)	25.4(3)	38.8(6)	20.6(5)	38.6(3)	21.0(0)
Total	101.1	98.3	100.6	98.8	101.1	98.1	100.3	97.2
Si	1.926(20)	0.021(10)	1.869(26)	0.017(1)	1.985(8)	0.012(3)	1.973(4)	0.013(1)
Al	0.127(26)	0.939(12)	0.255(38)	1.569(38)	0.034(6)	0.345(13)	0.042(9)	0.373(6)
Cr	0.052(9)	1.044(9)	0.043(7)	0.426(37)	0.039(6)	1.667(14)	0.042(4)	1.624(5)
Mg	1.879(17)	0.984(8)	1.814(19)	0.974(4)	1.920(14)	0.958(9)	1.927(11)	0.978(4)
Total	3.984(6)	2.988(3)	3.981(5)	2.986(1)	3.978(6)	2.982(2)	3.984(2)	2.988(2)

P (kbar)	20		15		20		10	
T (°C)	1400		1400		1400		1400	
Cr # (bulk)	20		10		10		50	
	OPX	SPI	OPX	SPI	OPX	SPI	OPX	SPI
	S 116-II	S 116-II	S 131	S 131	S 130	S 130	S 50	S 50
SiO_2	56.1(7)	0.6(1)	55.5(8)	1.2(6)	55.0(5)	0.8(3)	58.7(7)	0.5(3)
Al_2O_3	5.7(9)	50.4(11)	6.6(8)	58.7(4)	7.7(8)	58.1(6)	2.2(3)	27.6(7)
Cr_2O_3	1.3(1)	22.2(17)	0.8(1)	10.4(1)	0.9(1)	10.5(5)	1.4(4)	46.9(7)
MgO	36.7(3)	25.4(2)	36.5(6)	26.5(2)	36.2(3)	26.3(5)	38.6(2)	23.1(2)
Total	99.8	98.6	99.4	96.8	99.8	95.7	100.9	98.1
Si	1.885(20)	0.016(2)	1.870(16)	0.030(15)	1.848(18)	0.021(8)	1.950(14)	0.015(8)
Al	0.227(34)	1.539(32)	0.261(33)	1.753(11)	0.304(30)	1.755(11)	0.088(11)	0.929(20)
Cr	0.035(3)	0.454(35)	0.022(4)	0.208(5)	0.024(4)	0.213(7)	0.036(11)	1.061(20)
Mg	1.836(11)	0.979(3)	1.835(22)	1.000(8)	1.812(15)	1.006(5)	1.914(16)	0.984(4)
Total	3.983(3)	2.988(1)	3.988(12)	2.991(4)	3.988(11)	2.995(3)	3.988(8)	2.989(3)

P (kbar)	10		10		5		5	
T (°C)	1400		1400		1400		1400	
Cr # (bulk)	20		80		80		90	
	OPX	SPI	OPX	SPI	OPX	SPI	OPX	SPI
	S 112-I	S 112-I	S 112-II	S 112-II	S 122-I	S 122-I	S 127-I	S 127-I
SiO_2	56.4(13)	0.5(1)	57.6(7)	0.3(0)	59.2(8)	0.4(0)	60.2(9)	0.4(1)
Al_2O_3	4.8(12)	51.3(39)	0.5(2)	9.7(2)	0.7(2)	10.7(2)	0.2(0)	5.7(3)
Cr_2O_3	1.3(3)	19.4(43)	1.1(1)	65.3(5)	1.4(2)	65.3(5)	1.1(1)	72.3(6)
MgO	37.0(10)	24.5(6)	37.7(5)	19.9(1)	39.2(5)	21.0(4)	39.8(6)	20.9(5)
Total	99.3	95.7	96.9	95.2	100.5	97.4	101.3	99.3
Si	1.901(32)	0.014(3)	1.990(7)	0.010(1)	1.978(9)	0.012(1)	1.992(4)	0.013(4)
Al	0.192(50)	1.597(93)	0.021(6)	0.367(4)	0.026(9)	0.391(6)	0.005(5)	0.210(6)
Cr	0.034(9)	0.407(94)	0.029(4)	1.653(3)	0.037(6)	1.609(10)	0.029(3)	1.788(18)
Mg	1.860(38)	0.966(7)	1.945(25)	0.950(6)	1.949(7)	0.976(8)	1.964(5)	0.977(15)
Total	3.987(13)	2.984(3)	3.985(10)	2.980(2)	3.990(4)	2.988(0)	3.990(2)	2.988(5)

P (kbar)	5		35		35			35	
T (°C)	1400		1500		1500			1500	
Cr # (bulk)	46		50		20			80	
	OPX	SPI	OPX	SPI	OPX	SPI	GAR	OPX	SPI
	S 127-III	S 127-III	S 51	S 51	S 117-I	S 117-I	S 117-I	S 117-II	S 117-II
SiO_2	59.1(2)	0.4(1)	55.0(4)	0.5(1)	55.4(7)	0.8(1)	43.7(1)	58.4(6)	0.6(1)
Al_2O_3	1.9(1)	28.7(13)	5.3(3)	29.4(7)	6.9(7)	47.0(34)	21.3(4)	1.2(3)	10.0(1)
Cr_2O_3	1.3(2)	45.6(18)	2.9(2)	44.9(8)	1.8(3)	24.9(38)	4.5(8)	2.0(5)	65.3(3)
MgO	39.3(3)	23.0(1)	36.9(1)	23.4(1)	36.0(3)	24.9(5)	29.6(8)	38.2(7)	21.0(2)
Total	101.6	97.7	100.1	98.2	100.1	97.6	99.1	99.8	96.9
Si	1.952(8)	0.012(2)	1.857(12)	0.015(2)	1.859(19)	0.021(2)	3.004(17)	1.966(11)	0.019(2)
Al	0.075(4)	0.967(43)	0.211(12)	0.983(20)	0.271(28)	1.463(84)	1.728(20)	0.047(11)	0.368(4)
Cr	0.033(6)	1.030(39)	0.076(6)	1.005(20)	0.048(8)	0.522(86)	0.245(43)	0.053(13)	1.618(5)
Mg	1.934(8)	0.980(5)	1.856(8)	0.988(3)	1.803(14)	0.982(3)	3.034(56)	1.918(26)	0.982(6)
Total	3.994(5)	2.989(1)	4.000(5)	2.991(1)	3.981(5)	2.988(1)	8.011(23)	3.984(10)	2.987(2)

Table 4 (Contd.)

P (kbar)	25		25		25		15	
T (°C)	1500		1500		1500		1500	
Cr # (bulk)	50		80		20		90	
	OPX S 47	SPI S 47	OPX S 113-I	SPI S 113-I	OPX S 113-II	SPI S 113-II	OPX S 124	SPI S 124
SiO_2	56.5(1)	0.7(1)	59.3(5)	0.5(1)	55.0(6)	0.7(1)	60.2(4)	0.4(0)
Al_2O_3	3.9(2)	26.8(2)	1.2(4)	9.4(2)	8.0(7)	49.6(7)	0.4(2)	5.2(4)
Cr_2O_3	2.3(1)	47.2(4)	1.8(3)	67.2(12)	1.7(2)	22.1(2)	1.6(2)	72.8(4)
MgO	38.2(2)	23.4(1)	37.5(3)	20.3(8)	35.1(5)	24.8(4)	39.5(2)	20.6(2)
Total	100.9	98.1	99.8	97.4	99.8	97.2	101.7	99.0
Si	1.889(4)	0.020(3)	1.991(11)	0.016(3)	1.849(15)	0.019(2)	1.986(7)	0.014(1)
Al	0.152(8)	0.904(10)	0.046(14)	0.349(7)	0.316(27)	1.536(4)	0.014(7)	0.191(14)
Cr	0.061(2)	1.070(5)	0.049(8)	1.665(14)	0.045(5)	0.459(6)	0.041(5)	1.813(16)
Mg	1.902(7)	0.999(1)	1.877(13)	0.948(21)	1.759(18)	0.971(4)	1.946(7)	0.966(5)
Total	4.004(3)	2.993(1)	3.963(3)	2.978(8)	3.969(4)	2.985(1)	3.987(3)	2.984(1)

P (kbar)	10	
T (°C)	1500	
Cr # (bulk)	50	
	OPX S 49	SPI S 49
SiO_2	57.3(8)	0.6(1)
Al_2O_3	2.8(8)	27.4(13)
Cr_2O_3	2.0(4)	46.5(11)
MgO	38.5(5)	23.1(2)
Total	100.6	97.6
Si	1.918(22)	0.017(4)
Al	0.111(32)	0.929(38)
Cr	0.052(10)	1.056(33)
Mg	1.919(21)	0.988(4)
Total	4.000(4)	2.990(2)

[a] Analyses of spinels yielded totals systematically lower than 100, although the structural values indicate high-quality analyses. Low totals can be caused by beam current fluctuations during the analyses. Another possibility to explain low totals in spinels might be lower conductivity of $Mg(Cr,Al)_2O_4$ spinels relative to orthopyroxene (N.G. Ware, personal communication), the latter of which yielded higher totals on average. Because of the strongly differing hardness of spinel, opx and olivine, polishing of the experimental specimens often resulted in proud spinel slightly sticking out of the surface. Proud minerals usually yield higher totals, as exited X-rays are less subject to attenuation on the way out of the sample into the detector. However, lower conductivity of the spinel would, in fact, counteract this effect, thus resulting in lower totals

Energy and wavelength dispersive analyses were obtained with a JEOL 6400 scanning electron microscope at the Electron Microscopy Unit (EMU) and with a Cameca "Microbeam" electron microprobe at the Research School of Earth Sciences, both at the Australian National University. All analyses were performed with a spot size of ~1 μm. Special care was taken in selecting areas of orthopyroxene to analyse, so as to avoid small spinel inclusions within the orthopyroxene.

Experimental results

As expected from equilibrium (1), the addition of Cr to the MAS system lowers the amount of alumina dissolved in the orthopyroxene solid solution at a specified pressure and temperature, as illustrated in Fig. 1 for runs at 24 kbar. A similar trend is observed at other pressures. The experimental and thermodynamic results in the Cr-free system (e.g. Gasparik and Newton 1984) indicate that the solubility of alumina in orthopyroxene depends on temperature, increasing temperature resulting in increasing alumina in orthopyroxene. The same trend is observed in the Cr-bearing system MAS–Cr (e.g. Fig. 1).

Figure 2 shows results from experiments at 1400 °C at pressures between 5 and 54 kbar. The alumina solubility in orthopyroxene seems also to depend slightly on pressure in the middle range of Al/(Al + Cr) ratios, with higher pressure, correlating with more alumina in the orthopyroxene at a given spinel composition.

Equilibrium (2) describes the partitioning of Cr and Al between spinel and orthopyroxene in MAS–Cr. Figure 3 depicts the partitioning as a function of temperature at a constant pressure of 24 kbar. The results indicate the temperature effect on equilibrium (2) is negligible. Figure 4 shows the results at a constant temperature (1400 °C), and pressures between 5 and 54 kbar. Within the error margins, no significant pressure effect on equilibrium (2) is observed either.

Two experiments in relatively low bulk Cr/(Cr + Al) compositions yielded garnet as an additional phase (S-117-I and S-111-II at 35 kbar, 1500 °C and 1400 °C respectively). The garnet compositions exhibit a relative large scatter. Taking the uncertainties into account, the garnet composition in both experiments is constant with a Cr/(Cr + Al) in the garnet of 0.12 ± 0.03.

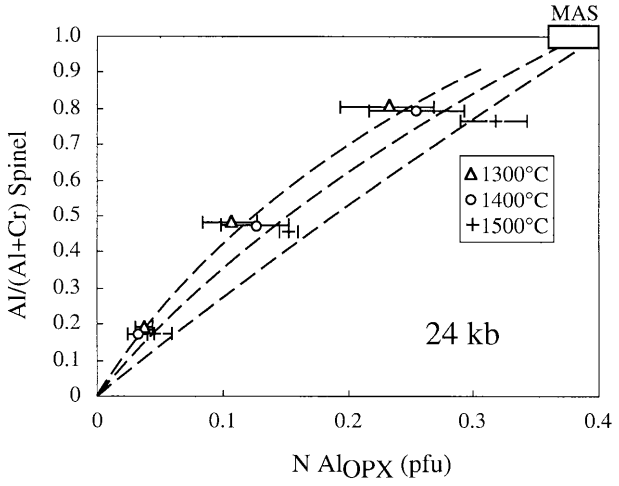

Fig. 1 The solubility of alumina in orthopyroxene in equilibrium with spinel and olivine. Experimental results at 24 kbar are depicted; experiments at other pressures show similar trends. The *bars* indicate maximum and minimum alumina contents in orthopyroxene (Table 4); uncertainties in spinel compositions are relatively small (Table 4) and are, for clarity, not shown here. Experiments between 1300 and 1500 °C are depicted. Note that experiments at 1300 and 1500 °C were performed at 25 kbar (cf. Table 3). The *box* in the right upper corner indicates experiments in the Cr-free system (MAS) by Gasparik and Newton (1984). The *lines* are hand-drawn to illustrate the observed trends of the experimental results. (N Al_{opx} (pfu) = alumina content in orthopyroxene per formula unit of six oxygens.) At 1300 °C and 24 kbar garnet is stable in the Cr-free system MAS

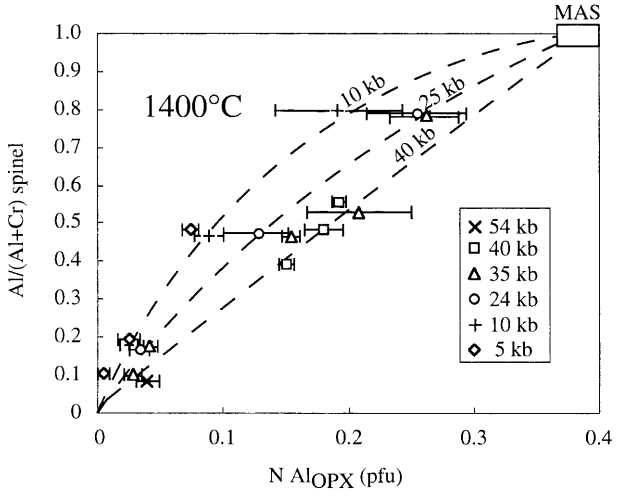

Fig. 2 Experiments in the system MAS–Cr at 1400 °C and pressures between 5 and 54 kbar. *Bars* indicate maximum and minimum alumina contents in orthopyroxene as determined by electron microprobe (cf. Table 4). Experiments at other temperatures exhibit similar trends. The amount of alumina solved in orthopyroxene is a function of the coexisting spinel composition and perhaps also of pressure. The depicted *lines* are hand-drawn to illustrate the possible pressure trends. (N Al_{opx} pfu = number of cations of Al in orthopyroxene per formula unit of six oxygens). The slight pressure effect on the solubility of alumina in orthopyroxene in the Cr-free system MAS is actually opposite to that observed in MAS–Cr. This results in an inversion of the slightly positive slope of the alumina isopleths in orthopyroxene in MAS to a slightly negative slope of the isopleths in relatively Cr-rich compositions

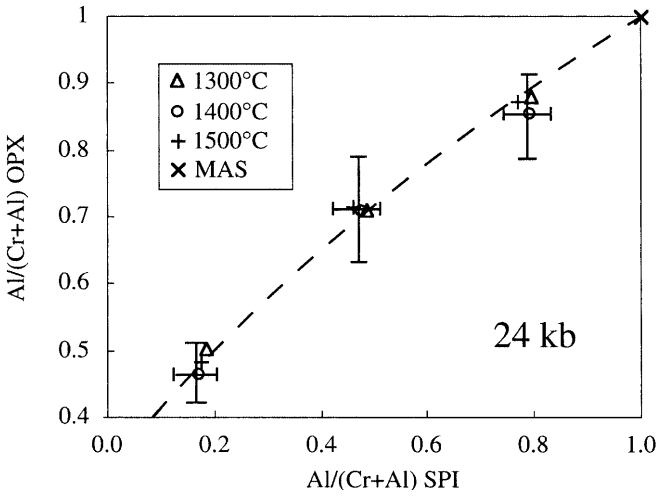

Fig. 3 Experimental results at 24 kbar and different temperatures. Note that experiments at 1300 and 1500 °C were performed at 25 kbar (cf. Table 3). The *cross* in the upper right corner depicts compositions in the Cr-free systems. For clarity, only uncertainties for the 1400 °C experiments (Table 4) are shown; other experiments show similar uncertainties. The *line* is hand-drawn

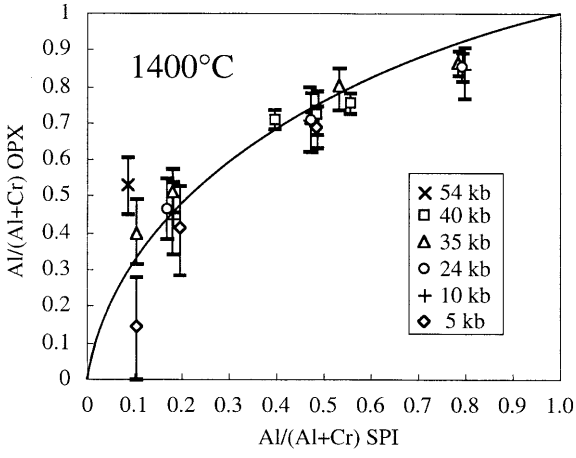

Fig. 4 Experimental results in MAS–Cr at 1400 °C and pressures ranging from 5 to 54 kbar. For clarity, only uncertainties are shown for the orthopyroxenes, especially as the errors in spinel compositions are comparatively small (Table 4). Compositions in the Cr-free system (MAS) lie in the upper right corner. All experiments but two (at 5 and 54 kbar) fall onto the curve

Thermodynamic evaluation of results

A number of solution models have been proposed to describe the mixing of $Mg_2Si_2O_6$–$MgAl_2SiO_6$ orthopyroxenes in the system MAS (e.g. Wood and Banno 1973; Ganguly and Ghose 1979; Lane and Ganguly 1980). In the most widely used model, Wood and Banno (1973) assumed that half the Al in the orthopyroxene formula unit of six oxygens substitutes for Mg on the M1 octahedral site, with the other half of the Al occupying an adjacent tetrahedral site. Since the position of the Al onto the tetrahedral site is completely specified by the

position in the crystal structure of the octahedral Al, the tetrahedral Al contributes nothing to the configurational entropy of mixing, which therefore corresponds to one-site mixing. Hence

$$a^{opx}_{(Mg_2Si_2O_6)} = 1 - (n_{Al}/2)$$

$$a^{opx}_{(MgAl_2SiO_6)} = (n_{Al}/2)$$

where n_{Al} is the number of Al cations per formula unit of six oxygens.

In the context of crystal-field theory, Cr^{3+} has the largest excess octahedral site preference energy of any first-row transition cation (Burns 1970, 1975), and is found exclusively in octahedral co-ordination in oxides and silicates (Burns and Burns 1975). Moreover, its ionic radius is considerably larger than that of Al^{3+}, hence much larger than that of Si^{4+}. Both these simple crystal-chemical considerations argue that Cr^{3+} should not substitute for Si on the tetrahedral sites of the orthopyroxene structure. Accordingly, a suitable end member to describe the thermodynamics of Cr^{3+} in orthopyroxenes might, one would suppose, be $MgCrAlSiO_6$, and not $MgCr_2SiO_6$ (e.g. Chatterjee and Terhart 1985).

The results presented here, however, confound this expectation. The most obvious point is that in several runs $n_{Al} < n_{Cr}$ is observed, hence the hypothetical end member $MgCrAlSiO_6$ cannot account for all the Cr^{3+}. Similarly, Canil and O'Neill (1996) have found $n_{Al} < (n_{Cr} + n_{Fe^{3+}})$ in natural orthopyroxenes.

Even more unexpected is that an extremely good fit to the partitioning of Cr^{3+} and Al between orthopyroxene and spinel is obtained if the partitioning reaction is written as:

$$\underset{\text{opx}}{1/2MgAl_2SiO_6} + \underset{\text{spinel}}{1/2MgCr_2O_4} = \underset{\text{opx}}{1/2MgCr_2SiO_6} + \underset{\text{spinel}}{1/2MgAl_2O_4} \quad (4)$$

and activities are modelled making the simplest possible assumption, that

$$a^{opx}_{(MgAl_2SiO_6)} = (n_{Al}/2)^2$$

and

$$a^{opx}_{(MgCr_2SiO_6)} = (n_{Cr}/2)^2$$

(i.e. ideal two-site mixing of Al and Cr). Assuming appropriate activity–composition relations for the spinel solid solution from previous work in the literature, the 37 data points from this study (Table 4) can be fitted very well to this model (the fitting procedure and results are described fully below). Including non-ideal terms for the orthopyroxene solid solution in the form of a ternary regular solution between $Mg_2Si_2O_6$, $MgAl_2SiO_6$ and $MgCr_2SiO_6$ did not improve the fit at all, implying $W^{opx}_{MC} = 0$, and $W^{opx}_{EM} = W^{opx}_{EC}$. The components used here are defined as $M = MgAl_2SiO_6$, $E = Mg_2Si_2O_6$, $C = MgCr_2SiO_6$, and the mole fractions of these components can be defined without ambiguity in terms of the number of Al and Cr cations per formula unit of six oxygens (n_{Al} and n_{Cr}) as:

$$X^{opx}_E = (1 - X^{opx}_M - X^{opx}_C) = (1 - n_{Al}/2 - n_{Cr}/2)$$

$$X^{opx}_M = n_{Al}/2$$

$$X^{opx}_C = n_{Cr}/2$$

Moreover, if W^{spinel}_{Al-Cr} is allowed to vary as a parameter in the regression, we find $W^{spinel}_{Al-Cr} \approx 10$ kJ mol^{-1} (on a one-site basis), which is in very good agreement with the value experimentally determined by Oka et al. (1984; and re-evaluated here in the Appendix), from completely independent measurements on the partitioning of Al and Cr between $Mg(Al, Cr)_2O_4$ spinel and $(Al, Cr)_2O_3$ solid solutions. This agreement is surely indicative that the simple two-site model, unlikely though it may appear from a crystal-chemical perspective, has real validity in a thermodynamic sense.

The next stage of the model-building process is to fit the experimental data of this study along with literature data in the systems MAS, CMAS and NCMAS to a thermodynamic expression for reaction (1). However, here a paradox is encountered. The simple two-site model used so successfully for reaction (2) is not able to fit these data satisfactorily, even if we use more complicated excess mixing models. If only the data from the Cr-free systems are considered, then although a fair fit, statistically speaking, can be obtained with the two-site model, this is only with an exceptionally large excess mixing term ($W^{opx}_{EM} \sim 200$ kJ mol^{-1}). Such a large value is physically unreasonable; more tangibly, it is also grossly inconsistent with the calorimetrically measured heats of mixing in the clinopyroxene join $CaMgSi_2O_6$–$CaAl_2SiO_6$ (Newton et al. 1977), expected to be somewhat similar to the $Mg_2Si_2O_6$–$MgAl_2SiO_6$ orthopyroxenes of interest here. This analogy implies that W^{opx}_{EM} should be ~20 kJ mol^{-1}.

In any case, no satisfactory fit with two-site mixing at all could be found when the MAS–Cr data were included. Our conclusion is that reaction (1) clearly requires a coupled-substitution for the orthopyroxene mixing model (equivalent to one-site mixing), of the type used by Wood and Banno (1973); yet, reaction (2) requires the two-site mixing model.

The solution to this paradox is to invoke a model in which there is random mixing of Mg, Al and Cr^{3+} on the M1 site, with complete coupling of (Al + Cr^{3+}) on M1 with (Al + Cr^{3+}) on the tetrahedral sites (i.e. as postulated for one-site mixing in the MAS system), but with random mixing of Al with Cr^{3+} on the "associated" tetrahedral site.

The configurational entropy of mixing in this model is:

$$S_{config} = -R\Big[\big(1 - X^{opx}_M - X^{opx}_C\big)\ln\big(1 - X^{opx}_M - X^{opx}_C\big) + X^{opx}_M \ln X^{opx}_M + X^{opx}_C \ln X^{opx}_C + X^{opx}_M \ln \frac{X^{opx}_M}{\big(X^{opx}_M + X^{opx}_C\big)} + X^{opx}_C \ln \frac{X^{opx}_C}{\big(X^{opx}_M + X^{opx}_C\big)}\Big]$$

The first three terms on the right hand side of this equation are due to the mixing of Mg, Al and Cr^{3+} on the octahedral (M1) site; the last two terms are due to the mixing of Al and Cr on the "associated" tetrahedral site.

Since the form of these last two terms is slightly different from that normally obtained for the configurational entropy of mixing on sites, we give their derivation explicitly, as follows: The permutability Ω of Al and Cr on the "associated" tetrahedral sites is

$$\Omega = (N_{Al} + N_{Cr})!/(N_{Al}! + N_{Cr}!)$$

where N_{Al} and N_{Cr} are the numbers of Al and Cr cations on those sites, per mole (six oxygen formula basis). The configurational entropy of mixing on these sites is:

$$\begin{aligned} S_{config} &= k \ln\ \Omega \\ &= k[\ln(N_{Al} + N_{Cr})! - \ln N_{Al}! - \ln N_{cr}!] \end{aligned}$$

where k is the Boltzmann constant. Using Stirling's approximation for large numbers (i.e. if x is a large number, $\ln x! = x \ln x - x$):

$$\begin{aligned} S &= -k[(N_{Al} + N_{Cr}) \ln(N_{Al} + N_{Cr}) - N_{Al} \ln N_{Al} - N_{Cr} \ln N_{Cr}] \\ &= -k\left[N_{Al} \ln \frac{N_{Al}}{(N_{Al} + N_{Cr})} + N_{Cr} \ln \frac{N_{Cr}}{(N_{Al} + N_{Cr})}\right] \end{aligned}$$

Hence, since $N_{Al} = NX_M^{opx}$ and $N_{Cr} = NX_C^{opx}$, where N is Avogadro's number,

$$S = -R\left[X_M \ln \frac{X_M}{X_M + X_C} + X_C \ln \frac{X_C}{X_M + X_C}\right], \quad \text{where } R = kN.$$

Differentiation of the equation for the configurational entropy of mixing gives the following expressions for the ideal part of the activities of each component:

$$a^{opx}_{Mg_2Si_2O_6} = (1 - X_M^{opx} - X_C^{opx})$$

$$a^{opx}_{MgAl_2SiO_6} = (X_M^{opx})^2/(X_M^{opx} + X_C^{opx})$$

$$a^{opx}_{MgCr_2SiO_6} = (X_C^{opx})^2/(X_M^{opx} + X_C^{opx})$$

This formulation is equivalent to two-site mixing for the ratio $a_{MgAl_2SiO_6}/a_{MgCr_2SiO_6}$ in modelling equilibrium (2), but reduces to one-site mixing between $Mg_2Si_2O_6$ and $MgAl_2SiO_6$ in the Cr-free system, as required by the data for equilibrium (1). With this model it was possible to fit 97 data from this study and from the literature in the systems MAS, CMAS, NCMAS and MAS–Cr satisfactory to equilibrium (1), while also fitting the MAS–Cr data to equilibrium (2).

In formulating the above model, we have implicitly assumed that the partitioning of Al and Cr between the octahedral M1 site and our hypothetical "associated" tetrahedral site is random. It is to be understood that the site assignments used here are only meant as a heuristic guide to formulating the algebra: we do not expect that an XRD experiment, for example, would reveal the presence of tetrahedral Cr^{3+} in these orthopyroxenes. In actuality, tetrahedral Cr^{3+} could be avoided if it is Mg^{2+} that occupies the tetrahedral site, with the Cr^{3+} replacing this Mg on the octahedral site. A similar substitution mechanism has been proposed for the Cr^{3+} substitution into the wadsleyite structure (Gudfinnsson and Wood 1998). Incorporation of such order–disorder effects into the model would introduce tremendous complexity that is in no way justified by any practical need as regards data fitting.

Details of the fitting procedure

Accurate activity–composition relations may in principle be determined from the analysis of coexisting solid solutions, but only if the activity–composition relations of one of the phases are known independently. Hence, the evaluation of the orthopyroxene solid solution depends on the spinel solid-solution model. Activity–composition relations in the $Mg(Al, Cr)_2O_4$ spinel solid solution have been calibrated from the partitioning of Al and Cr between this phase and $(Al, Cr)_2O_3$, studied by Oka et al. (1984). Interpretation of Oka et al.'s data in turn depends on the mixing properties of the $(Al, Cr)_2O_3$ solid solution, which were evaluated by Chatterjee et al. (1982) from the experimental work of Jacob (1978). The Appendix presents a critical re-evaluation of this chain of investigation. We find that while both the $(Al, Cr)_2O_3$ and the $Mg(Al, Cr)_2O_4$ solid solution are obviously non-ideal, it is difficult to decide whether the non-ideality can be modelled with symmetrical excess mixing models (the simplest possible representation of non-ideality in a solid solution), or whether the more complicated asymmetric mixing models are warranted. Accordingly, both possible models have been investigated here. In summary, these models are:

A: a symmetric model for both the $Mg(Al, Cr)_2O_4$ and the $(Al, Cr)_2O_3$ solid solutions
B: an asymmetric model for both the $Mg(Al, Cr)_2O_4$ and the $(Al, Cr)_2O_3$ solid solutions

With these models for the spinel solid solution, the 37 data of the present study were then fitted by non-linear least squares regression to equations of the form:

$$0 = \Delta H_2 - T\Delta S_2 P + RT \ln\left[\frac{X_{Al}^{spinel}}{X_{Cr}^{spinel}} \frac{X_C^{opx}}{X_M^{opx}}\right] + RT \ln \gamma_{Cr}^{spinel} - RT \ln \gamma_{Al}^{spinel}$$

The compositional data were weighted according to the uncertainties given in Table 4, and the uncertainties on P were assumed to be ± 1 kbar and on T ± 15 K (1 SD).

For model A (symmetric spinel mixing model) we obtain:

$$\begin{aligned} \text{A}: \Delta G(2) \ &= 19,065\,(10,351) - 17.06\,(5.90)\,T \\ &\quad - 0.154\,(0.047)\,P \text{ J mol}^{-1} \end{aligned}$$

with a reduced chi-squared (χ^2_ν) of 0.76, while model B (asymmetric spinel model) yields

$$\begin{aligned} \text{B}: \Delta G(2) \ &= 21,443\,(10,501) - 18.67\,(5.99)\,T \\ &\quad - 0.161\,(0.048)\,P \text{ J mol}^{-1} \end{aligned}$$

with $\chi^2_\nu = 0.72$. P is in bars. The numbers in parentheses indicate the uncertainties of the individual parameters as

determined by the regressions. The low values of χ^2_ν indicate that both models fit the data well. Only two runs are not fitted within two standard deviations of their observed uncertainties (S 126 – 54 kbar, S 127-III – 5 kbar, see Fig. 4).

We then fitted equilibrium (1) using both the symmetric and the asymmetric model for the spinel solid solution. We used 60 data from the literature for the Cr-free systems MAS (Dankwerth and Newton 1978; Gasparik and Newton 1984), CMAS (Gasparik 1984; Sen 1985; Klemme 1998; Klemme and O'Neill 2000) and NCMAS (Walter and Presnall 1994), plus the 37 data for the system MAS–Cr from this study. All data were fitted simultaneously to the equation:

$$\begin{aligned}0 = {} & \Delta H_1 - T\Delta S_1 + \Delta V_1 P \\ & + RT\left[\ln(1 - X_M^{opx} - X_E^{opx}) - 2\ln X_M^{opx} + \ln(X_M^{opx} + X_C^{opx}) + 2\ln X_{Al}^{spinel}\right] \\ & + 2RT\ln\gamma_{Al}^{spinel} + W_{EM}^{opx}(-1 + 2X_M^{opx} + X_C^{opx}) + W_{EC}^{opx} X_C^{opx}\end{aligned}$$

Where possible, the data were weighted according to the published uncertainties in mineral compositions (Danckwerth and Newton 1978; Sen 1985; Walter and Presnall 1994; Klemme 1998). However, the uncertainties were not given by Gasparik (1984) and Gasparik and Newton (1984), so that uncertainties for n_{Al}^{opx} of ± 0.005 (Al atoms per formula unit of six oxygens) were assumed. Note that from the modelling of reaction (2) above, we constrain $W_{EC}^{opx} = W_{EM}^{opx}$, $W_{MC}^{opx} = 0$.

In performing the non-linear least-squares regression, we found that allowing the value of $W_{EM}^{opx} (= W_{EC}^{opx})$ to vary in the usual way resulted in lack of convergence, probably because this parameter is highly correlated with others over the relatively limited range of Mg–Al compositional space which is accessible in orthopyroxene solid solutions. Hence we constrained the value of this parameter to be $W_{EM}^{opx} = W_{EC}^{opx} = 20$ kJ mol^{-1}, by analogy with the calorimetric data for $CaMgSi_2O_6$–$CaAl_2SiO_6$ clinopyroxenes (Newton et al. 1977). Manual adjustment of W_{EM}^{opx} to higher or lower values increases reduced chi-squared for model A, indicating that the chosen value of 20 kJ mol^{-1} was appropriate to a surprising degree of precision. The results for the two models are as follows. Model A [symmetric model for Mg(Al, Cr)$_2$O$_4$ spinels]:

$$\Delta G\,(1) = 188\,(312) - 4.518\,(0.216)\,T - 0.018\,(0.007)\,P \text{ J mol}^{-1}$$

with a reduced chi-squared of 1.93. P is in bars; and model B [asymmetric model for Mg(Al, Cr)$_2$O$_4$ spinels]

$$\Delta G\,(1) = 1363\,(300) - 4.890\,(0.206)\,T - 0.014\,(0.0006)\,P \text{ J mol}^{-1}$$

with a reduced chi-squared of 2.21. For this model B we used $W_{EM}^{opx} = 21$ kJ mol^{-1} since this value gave a slightly better fit. Nevertheless, the value of χ^2_ν is clearly greater than for model A.

Since model A is also the simpler model, it seems on balance preferable, although it does give a poorer fit to some of the Mg(Al, Cr)$_2$O$_4$ and (Al, Cr)$_2$O$_3$ data (see Appendix).

Again, the same two data (S 126 at 54 kbar, and S 127-III at 5 kbar) which were poorly fit to equilibrium (2) were also poorly fit to equilibrium (1). One datum of Sen (1985) in the system CMAS does not fit well either (15 kbar, 1200 °C). Also, the recent experimental results of Gudfinnsson and Presnall (1996) in the system CMAS could not be fitted within their stated uncertainties and were therefore excluded from the fitting procedure. These data differ from the earlier data from the same laboratory of Walter and Presnall (1994), which agree well with the other studies.

Discussion and implications

Previous work

In an early experimental study, Dickey and Yoder (1971) investigated the distribution of Cr and Al between coexisting clinopyroxene and spinel in the system CMAS-Cr, focusing on the spinel compositions as a function of temperature above the solidus. Perhaps due to short run times spinels were only small (< 3 μm), and the clinopyroxene was reported to host numerous spinel inclusions. Wood (1978) investigated the influence of Cr on the transition from spinel to garnet peridotite in the system MAS–Cr. Evaluation of his experiments led him to the assumption of ideal two-site mixing of the $MgAl_2O_4$–$MgCr_2O_4$ solid solution. In a subsequent study on the transition in the system CMAS–Cr, O'Neill (1981) postulated a positive deviation from ideality on the binary $MgAl_2O_4$–$MgCr_2O_4$ join. Oka et al. (1984) investigated the partitioning between Cr and Al between the (Al, Cr)$_2$O$_3$ and the Mg(Al, Cr)$_2$O$_4$ solid solutions in detail, and showed that the spinel solution does indeed deviate positively from ideality, in agreement with O'Neill's (1981) prediction. Carroll-Webb and Wood (1986) studied the partitioning of Cr and Al between coexisting spinel and sodic clinopyroxene of formula Na(Al, Cr)Si_2O_6. They performed reversal piston-cylinder experiments at 25 kbar and 1100 °C (two experiments at 1000 °C) on the partitioning equilibrium:

$$\underset{\text{clinopyroxene}}{NaCrSi_2O_6} + 1/2\,\underset{\text{spinel}}{MgAl_2O_4} = 1/2\,\underset{\text{spinel}}{MgCr_2O_4} + \underset{\text{clinopyroxene}}{NaAlSi_2O_6}$$

Caroll-Webb and Wood (1986) found that mixing in Na(Cr,Al)Si_2O_6 clinopyroxene was approximately ideal, which agrees well with the ideal mixing of the $MgAl_2SiO_6$ and $MgCr_2SiO_6$ components postulated in this study. Nickel (1986) investigated phase relations in the system CaO–MgO–Al_2O_3–SiO_2–Cr_2O_3. He found a good positive correlation of the Al/(Al + Cr) ratios of orthopyroxene and spinel (Nickel 1983), with no significant pressure or temperature effect, in good agreement with results of this study.

The only other experiments that can be directly compared with the results of this study are those reported in a recent paper by Doroshev et al. (1997). They investigated the partitioning of Cr and Al between

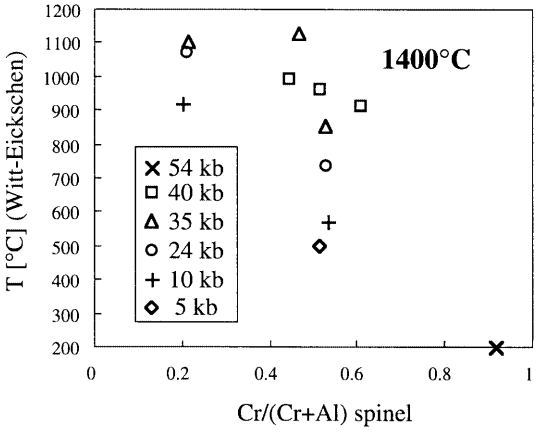

Fig. 5 Calculated temperature using the empirical geothermometer of Witt-Eickschen and Seck (1991) for experiments at 1400 °C in MAS–Cr of the present study. Witt-Eickschen and Seck's (1991) thermometer does not reproduce experiments in MAS (Gasparik and Newton 1984), it also cannot reproduce the present experimental results. Especially at high Cr/(Cr + Al) ratios, Witt-Eickschen and Seck's geothermometer (1991) systematically underestimates the experimental temperatures by several hundred degrees

coexisting spinel, orthopyroxene, olivine and garnet in the divariant field of the system MgO–Al_2O_3–SiO_2–Cr_2O_3 where garnet and spinel coexist with orthopyroxene and olivine. An attempt to fit Doroshev et al.'s (1997) data in conjunction with the present experimental results was not successful, indicating that their results are not compatible with ours. The large scatter in the orthopyroxene compositions as indicated by Doroshev et al. (see their comments on p 570 of their paper), may indicate failure to reach equilibrium, probably due to short run durations (e.g. only 24 h at 1400 °C as opposed to ~120 h at 1400 °C in the present study).

Geothermometry based on the solubility of alumina in orthopyroxene

Equilibrium (1) has been calibrated empirically by Witt-Eickschen and Seck (1991) as a geothermometer, using data for coexisting phases in spinel lherzolite xenoliths from West Eifel, Germany, with temperatures of equilibration of the xenoliths derived from the two-pyroxene geothermometer of Brey and Köhler (1990).

Here, we can use our experimental data to test this calibration. The temperatures calculated using the geothermometer of Witt-Eickschen and Seck (1991) for experiments at 1400 °C are plotted against the Cr/(Cr + Al) ratio of the spinel in Fig. 5. There is obviously poor agreement, especially at high Cr/(Cr + Al) ratios. This illustrates well the importance of including the effect of Cr in modelling any equilibrium involving aluminous pyroxenes.

Calculations of the position of the transition from garnet lherzolite to spinel lherzolite, for example, depend not only on the thermodynamics of Cr-garnets and Cr-spinels (Klemme and O'Neill 1997; Klemme et al. 2000), but also on the thermodynamics of Cr in pyroxenes (Asimov et al. 1995; Klemme 1998). The present study sets the stage for further investigations of phase relations in Cr-bearing systems relevant for the Earth's upper mantle.

Acknowledgments SK would like to acknowledge funding by an ANU PhD scholarship. The authors would also like to thank Drs C. Shaw and B. J. Wood for careful reviews which helped considerably to improve the manuscript. We would also like to thank members of the Petrochemistry and Experimental Petrology group at the Research School of Earth Sciences, especially Alan Major, Paul Willis, Dean R. Scott and William O. Hibberson.

Appendix

Activity–composition relations in Al–Cr solid solutions

Cr^{3+} can replace Al in octahedral co-ordination in many minerals, and complete solid solution exists between, for example, the oxides Al_2O_3–Cr_2O_3 [albeit with a solvus below ~950 °C (Roy and Barks 1972)]; spinels M Al_2O_4–M Cr_2O_4, where M is Mg, Fe^{2+}, Zn etc. (O'Neill and Navrotsky 1984); garnets $Ca_3Al_2Si_3O_{12}$–$Ca_3Cr_2Si_3O_{12}$ (Huckenholz and Knittel 1975) and $Mg_3Al_2Si_3O_{12}$–$Mg_3Cr_2Si_3O_{12}$ (Irifune and Hariya 1983; Doroshev et al. 1997); and clinopyroxenes $NaAlSi_2O_6$–$NaCrSi_2O_6$ (Carroll-Webb and Wood 1986). However, Cr^{3+} generally does not replace Al on tetrahedral sites. For example, the amounts of Cr substituting in $CaAl_2Si_2O_8$ (anorthite) are generally too small to be reported even when the anorthite-rich plagioclase is in equilibrium with Cr-rich spinel (e.g. Deer et al. 1992).

Approximate activity–composition relations in $Ca_3Al_2Si_3O_{12}$–$Ca_3Cr_2Si_3O_{12}$ garnet solutions were determined by Mattioli and Bishop (1984), by displacement of the univariant reaction:

$$Ca_3Al_2Si_3O_{12} + SiO_2 = CaAl_2Si_3O_8 + 2CaSiO_3$$

They found the solution to be nearly ideal, in agreement with the almost negligible excess enthalpies of solution found by Wood and Kleppa (1984) from oxide melt solution calorimetry.

More precise activity–composition relations in Al–Cr oxide and silicate solid solutions may in principle be determined from analysis of coexisting solid solutions. However, as has been shown for Fe^{2+}–Mg solid solutions, such measurements can only accurately yield the difference in the activity–composition relations of the two phases (e.g. Matsui and Nishizawa 1974; von Seckendorff and O'Neill 1993): it is necessary for absolute values of one of the phases to be known independently. Fortunately, such measurements exist for the Al_2O_3–Cr_2O_3 solid solution. Jacob (1978) determined the mixing properties of this solution from the displacement of the reaction:

$$2\ Cr + 1.5\ O_2 = Cr_2O_3$$

in fO_2–T space, using an electromotive force (emf) method with YDT (yttria-doped thoria) solid oxygen-specific electrolytes. The low fO_2 of the Cr–Cr_2O_3 equilibrium is beyond the useful range of zirconia-based electrolytes. The thoria-based electrolytes are difficult to obtain (they appear to be no longer manufactured commercially), and are also extremely expensive. Consequently, it is unlikely that Jacob's (1978) experiments will be repeated.

Jacob's experimental results were reinterpreted by Chatterjee et al. (1982), who fitted them to a subregular (asymmetric) solution model. Chatterjee et al. (1982) also reported molar volumes for the $(Al, Cr)_2O_3$ solution. This modelling was then used by Oka et al. (1984) in conjunction with their experimental partitioning data on coexisting $(Al, Cr)_2O_3$–$Mg(Al, Cr)_2O_4$ solid solutions at 25 kbar, to derive activity–composition relations for the latter solution. They found that the $Mg(Al, Cr)_2O_4$ spinel solid solution shows slightly asymmetric positive deviations from ideality. However, the

uncertainties (i.e. standard deviations) were not given by Chatterjee et al. (1982) or by Oka et al. (1984); indeed, nor were the details of the regression method they used. In view of the importance of the solution properties of $Mg(Al, Cr)_2O_4$ spinels to the interpretation of the experimental data of this study, the data fitting of these studies have been reexamined in detail.

Activity–compositions in $(Al, Cr)_2O_3$ solid solutions

Jacob (1978) studied seven compositions (nominal X_{Cr} from 0.1 to 0.9 using cells of the type:

$$Pt,\ (Al, Cr)_2O_3 + Cr|YDT|Cr_2O_3 + Cr, Pt$$

The temperature range was 800 to 1320 °C. Results were given only in the form of an equation for the emf of the cell, E (in millivolts). Here, we have refitted Jacob's results as follows. The emf at 1173 K (a temperature near the middle of the range studied, and close to the optimum for this type of experiment, according to Pownceby and O'Neill 1994a) was fitted to an equation of the form $3\,FE = \Delta\bar{G}_{mix} = RT \ln X_{Cr} + [AG_0 + AG_1\,(4\,X_{cr} - 1)\ldots]$ where the terms in AG_0 etc. are the terms in the Redlich–Kister expansion, F is the Faraday constant (96,484.56 J C^{-1}) and R the gas constant. The data were weighted assuming an uncertainty, one standard deviation, of 0.4 to 0.7 mV in E (Jacob 1978, his Table 1), and of ± 0.01 in X_{Cr}. The latter is assumed, as no uncertainty in composition is given by Jacob (1978). This is unfortunate, as in these type of experiments it is the uncertainties in composition which generally predominate.

For a one-term model (i.e. a symmetric or regular solution), $AG_0 = 19{,}390 \pm 690$ J mol^{-1} with a reduced chi-squared (χ^2_v) of 2.57. For the two-term model (asymmetric or subregular), $AG_0 = 20{,}200 \pm 700$ and $AG_1 = -2880 \pm 1100$ J mol^{-1}, with $\chi^2_v = 1.48$, i.e. seemingly a significantly better fit. Calculated values of X_{Cr} from these two fits are compared to their nominal values in Table A.1. It may be seen that the better fit of the two-term (subregular) model is entirely due to one composition, that at $X_{Cr} = 0.64$ (nominal), and even for the asymmetric model, the fit to this datum is relatively poor.

The calculated values of X_{Cr} for each model were then used as the input values in the regression to determine the temperature dependence of the mixing parameters AG_0 ($\pm AG_1$), i.e. the excess entropies of mixing, from the slopes dE/dT of the emf of the cells. The uncertainty in the slopes was assumed to be the uncertainty in the emf for each cell as given by Jacob (1978), divided by 400 K, the typical temperature range over which the cells were studied. For the one-term model, $AS_0 = 1.53 \pm 0.4$ J mol^{-1} K^{-1}, while for the two-term model, $AS_0 = 2.10 \pm 0.39$ and $AS_1 = 1.09 \pm 0.60$ J mol^{-1} K^{-1}.

The molar volumes of $(Al, Cr)_2O_3$ solutions measured by Chatterjee et al. (1982) were fitted to quadratic and cubic expressions in X_{Cr}, corresponding to the symmetric (regular) and asymmetric (subregular) solution models respectively, weighting the data according to the uncertainties in volume given by Chatterjee et al. (1982, their Table 1). However, Chatterjee et al. (1982) report their uncertainties in composition as standard errors of the mean, rather than as standard deviations. Standard errors of the mean tend to underestimate the true uncertainties in composition, probably because it is doubtful whether the parent population of compositions being sampled by a set of analyses is really completely homogenous. It is therefore preferable to use standard deviations, which were assumed to be three times the reported standard errors of the mean (as would be the case if the latter were based on ten analyses).

With this weighting,

$$V/cm^3 = 25.578 + 3.634\,X_{Cr} - 0.158\,X^2_{Cr}, \chi^2 v = 2.16$$

or

$$V/cm^3 = 25.578 + 3.795\,X_{Cr} - 0.629\,X^2_{Cr} - 0.311\,X^3_{Cr}, \chi^2 v = 1.13$$

Hence, for each g-atom of Al, Cr mixing, $AV_0 = 0.0079$ J bar^{-1} (symmetric model) or $AV_0 = 0.0081$ and $AV_1 = -0.0078$ J bar^{-1}. These numbers are slightly different from those given by Chatterjee et al. (1982), because the latter used a simplified regression method with unweighted data.

In summary: for a one-term, regular (symmetric) solution model:

$$AG_0 (= W^{sp}_{Al-Cr}) = 17{,}300 + 1.53\,T + 7.9\,P$$

with an uncertainty of ~700 J mol^{-1}.

For a two-term, subregular (asymmetric) model:

$$AG_0 = 17{,}320 + 2.10\,T + 8.1\,P$$

$$AG_1 = -1380 - 1.09\,T - 7.8\,P$$

where P is in kbar. The effect of pressure is obviously quite minor.

Activity–compositions in $Mg(Al, Cr)_2O_4$ spinel solutions

Oka et al. (1984) measured the partitioning of Al and Cr between $(Al, Cr)_2O_3$ and $Mg(Al, Cr)_2O_4$ solutions at 796, 1050 and 1250 °C. Compositions were determined from lattice parameters (see below). The uncertainties in X_{Cr} for the $Mg(Al, Cr)_2O_4$ solid solutions are quoted as 0.0091, 0.0022 and 0.0015 at 796, 1050 and 1250 °C respectively, while those for X_{Cr} in the $(Al, Cr)_2O_3$ solution are 0.0200, 0.0172 and 0.0028. Thus the composition of the $(Al, Cr)_2O_3$ oxide solution is quoted as being nearly an order of magnitude more precise at 1250 °C than at the other two temperatures. The scatter of the data at 1250 °C shows that this level of precision is over-optimistic. Therefore, to lessen the domination of these data in the regression analysis, their uncertainty in X_{Cr} was doubled to 0.0056.

With these uncertainties, the results of Oka et al. (1984) were fit by least squares regression in two ways, according to which model (symmetric or asymmetric) was assumed for the $(Al, Cr)_2O_3$ solution. For the asymmetric model, the regression gives:

$$\Delta H = 1015 \pm 710 \text{ J mol}^{-1}$$

$$\Delta S = 0.341 \pm 0.460 \text{ J mol}^{-1}$$

$$AG_0 = 12{,}400 \pm 260 \text{ J mol}^{-1}$$

$$AG_1 = -4963 \pm 450 \text{ J mol}^{-1}$$

with $\chi^2_v = 1.72$. The entropy of the exchange reaction is thus predicted to be approximately zero. No improvement to the fit was observed if the excess mixing parameters were allowed to vary as a function of temperature. For the symmetric model:

$$\Delta H = -6992 \pm 1524 \text{ J mol}^{-1}$$

$$\Delta S = -4.101 \pm 0.985 \text{ J mol}^{-1}$$

$$AG_0 = 9980 \pm 275 \text{ J mol}^{-1}$$

with $\chi^2_v = 1.07$, i.e. a significantly better fit to the data. In principle, the difference in standard entropies of the exchange reaction between the two models could also be used to discriminate between them, but at the moment the uncertainty in the entropy of $MgAl_2O_4$ is too large for this to be practical, due to the uncertainty in

Table A.1

X_{Cr} nom	X_{Cr} calc 1-term	X_{Cr} calc 2-term
0.1	0.1132	0.0968
0.24	0.2463	0.2386
0.37	0.3707	0.3751
0.5	0.4982	0.5094
0.64	0.6057	0.6181
0.77	0.7707	0.7774
0.9	0.9017	0.9032

the contribution from the configurational entropy of Mg–Al order–disorder.

$Mg(Al, Cr)_2O_4$ lattice parameters and molar volumes of mixing

Oka et al. (1984) also measured the lattice parameters across the $MgAl_2O_4$–$MgCr_2O_4$ solid solution, and hence derived molar volumes of mixing at room temperature. The interpretation of their data is complicated by the fact that the lattice parameter of $MgAl_2O_4$ depends on the amount of Mg/Al order–disorder, as well as the exact stoichiometry (i.e. bulk Mg/Al ratio), which can vary widely in this spinel. [By contrast, $MgCr_2O_4$ spinel shows negligible Mg/Cr order–disorder, and does not deviate significantly from the ideal stoichiometry, provided that the sample is synthesized somewhere within the broad range of oxygen fugacities where neither Cr^{2+} or Cr^{4+} is stable (O'Neill and Dollase 1994).] Oka et al. (1984) thus found that samples quenched from different temperatures have slightly different lattice parameters, which they ascribed to differing degrees of Mg/Al order. However, it is doubtful whether the difference between the equilibrium cation distributions at 1250 °C or 1050 °C and 796 °C would be preserved during the quench (O'Neill 1997), since rates of Mg–Al exchange appear to be fast on typical quenching time scales. It is therefore probable that the low value of the lattice parameter that they observed is instead due to the Mg/Al ratio in their $MgAl_2O_4$-rich spinels being slightly less than unity. This asymmetry appears to be largely due to a slightly low value for the lattice parameter of $MgAl_2O_4$, e.g. 8.0810 (1) Å at 1250 °C, as compared to that given by O'Neill (1997):

$$a_o/\text{Å} = 7.9829 + 0.1052(X_{MgO}/X_{Al_2O_3}) - 4.01 \times 10^{-6}\ T/K$$

where T is the temperature from which the sample was quenched, and all values refer to room temperature measurements. The value of the lattice parameter of $MgCr_2O_4$ measured by Chatterjee et al. (1982) is identical to that given by O'Neill and Dollase (1994), so there seems to be no interlaboratory bias. Hence stoichiometric $MgAl_2O_4$ quenched from 1250 °C should have a lattice parameter of 8.0820 Å. However, as mentioned above, slightly non-stoichiometric $MgAl_2O_4$ re-orders extremely rapidly on quenching, such that it is likely that the sample synthesized by Chatterjee et al. (1982) at 1250 °C has a cation distribution corresponding to an equilibration temperature of ~800 °C. The lattice parameter of stoichiometric $MgAl_2O_4$ at 800 °C is 8.0837 Å.

Because of these problems, the molar volume data of Chatterjee et al. (1982) were fitted without the datum for pure $MgAl_2O_4$. (Although we acknowledge that Mg–Al cation ordering may also be important in the more Al-rich members of the solid solution series, thermodynamic modelling indicates that it becomes rapidly less so as Cr replaces Al, hence all other data were accepted.) A satisfactory fit to a quadratic equation was obtained, with:

$$V(\text{J bar}^{-1}) = 3.9780 + 0.3983\ X_{Cr} - 0.01919(X_{Cr})^2$$

with chi-squared = 2.31. Hence W_V *Al–Cr (sp)* = 0.0096 J bar^{-1} per mole of Al–Cr. A slightly better fit is obtained using a cubic (i.e. asymmetric fit), with chi-squared = 1.95. However, examination of the fit shows that this is probably an artefact of the slightly lower lattice parameters of the most Al-rich data, as discussed above.

Hence $W^{sp}_{Al-Cr} = 9739 + 9.6\ P$ J mol^{-1}, where P is in kbar.

References

Ai Y (1992) Major and minor element systematics in the lherzolite system: a petrological and experimental study. PhD Thesis, Univ Tasmania

Asimov PD, Hirschmann MM, Ghiorso MS, O'Hara MJ, Stolper EM (1995) The effect of pressure induced solid–solid phase transitions on decompression melting of the mantle. Geochim Cosmochim Acta 59: 4489–4506

Bose K, Ganguly J (1995) Quartz–coesite transition revisited: reversed experimental determination at 500–1200 °C and retrieved thermochemical properties. Am Mineral 80: 231–238

Boyd FR, England JL (1960) Apparatus for phase-equilibrium measurements at pressures up to 50 kbar and temperatures up to 1750 °C. J Geophys Res 65: 741–748

Brey GP, Köhler T (1990) Geothermobarometry in four-phase lherzolites II. New thermobarometers, and practical assessment of existing thermobarometers. J Petrol 31: 1353–1378

Brodowsky H, Ketzner M, Krey C (1998) The influence of Al or B on the thermoelectric power of Pt/Pt–Rh thermocouples. Z Metallkunde 89: 518–521

Burns G, Hurst W (1972) Studies of the performance of W–Re thermocouples. In: Plumb HH (ed) Temperature, its measurement and control in science and industry. Instrument Society of America, Pittsburgh, pp 1751–1766

Burns RG (1970) Crystal field spectra and evidence of cation ordering in olivine minerals. Am Mineral 55: 1608–1632

Burns RG (1975) On the occurrence and stability of divalent chromium in olivines included in diamonds. Contrib Mineral Petrol 51: 213–221

Burns VM, Burns RG (1975) Mineralogy of chromium. Geochim Cosmochim Acta 39: 903–910

Canil D, O'Neill HStC (1996) Distribution of ferric iron in some upper-mantle assemblages. J Petrol 37: 609–635

Caroll-Webb SA, Wood BJ (1986) Spinel–pyroxene–garnet relationships and their dependence on Cr/Al ratio. Contrib Mineral Petrol 92: 471–480

Chatterjee ND, Terhart L (1985) Thermodynamic calculation of peridotite phase relations in the system MgO–Al_2O_3–SiO_2–Cr_2O_3, with some geological applications. Contrib Mineral Petrol 89: 273–284

Chatterjee ND, Leistner H, Terhart L, Abraham K, Klaska R (1982) Thermodynamic mixing properties of corundum–eskolaite, α-$(Al, Cr^{3+})_2O_3$, crystalline solutions at high temperatures and pressures. Am Mineral 67: 725–735

Danckwerth PA, Newton RC (1978) Experimental determination of the spinel peridotite to garnet peridotite reaction in the system MgO–Al_2O_3–SiO_2 in the range 900–1100 °C and Al_2O_3 isopleths of enstatite in the spinel field. Contrib Mineral Petrol 66: 189–201

Deer WS, Howie RA, Zussman J (1992) An introduction to the rock-forming minerals. Longman, Harlow

Dickey JS Jr, Yoder HS Jr (1971) Partitioning of chromium and aluminum between clinopyroxene and spinel. Carnegie Inst Wash Yearb 70: 384–392

Doroshev AM, Brey GP, Girnis AV, Turkin AI, Kogarko LN (1997) Pyrope–knorringite garnets in the earth's mantle: experiments in the MgO–Al_2O_3–SiO_2–Cr_2O_3 system. Russ Geol Geophys 38: 559–586

Fujii T (1977) Pyroxene equilibria in spinel lherzolite. Carnegie Inst Wash Yearb 76: 569–572

Ganguly J, Ghose S (1979) Aluminous orthopyroxene: order–disorder, thermodynamic properties, and petrologic implications. Contrib Mineral Petrol 69: 375–385

Gasparik T (1984) Two-pyroxene thermobarometry with new experimental data in the system CaO–MgO–Al_2O_3–SiO_2. Contrib Mineral Petrol 87: 87–97

Gasparik T, Newton RC (1984) The reversed alumina contents of orthopyroxene in equilibrium with spinel and forsterite in the system MgO–Al_2O_3–SiO_2. Contrib Mineral Petrol 85: 186–196

Glawe G, Szaniszlo A (1972) Long term drift of some noble- and refractory-metal thermocouples at 1600 K in air, argon and vacuum. In: Plumb HH (ed) Temperature, its measurement and control in science and industry. Instrument Society of America, Pittsburgh, pp 1645–1662

Gudfinnsson GH, Presnall DC (1996) Melting relations of model lherzolite in the system CaO–MgO–Al_2O_3–SiO_2 at 2.4–3.4 GPa and the generation of komatiites. J Geophys Res 101(B12): 27701–27709

Gudfinnsson GH, Wood BJ (1998) The effect of trace elements on the olivine–wadsleyite transformation. Am Mineral 83: 1037–1044

Huckenholz HG, Knittel D (1975) Uvarovite: stability of uvarovite–grossularite solid solutions at low pressure. Contrib Mineral Petrol 49: 211–232

Irifune T, Hariya Y (1983) Phase relationships in the system $Mg_3Al_2Si_3O_{12}$–$Mg_3Cr_2Si_3O_{12}$ at high pressure and some mineralogical properties of synthetic garnet solid solutions. Mineral J 11: 269–281

Jacob KT (1978) Electrochemical determination of activities in Cr_2O_3–Al_2O_3 solid solution. J Electrochem Soc 125: 175–179

Johannes W, Bell PM, Mao HK, Boettcher AL, Chipman DW, Hays JF, Newont RC, Seifert F (1971) An interlaboratory comparison of piston-cylinder pressure calibration using the albite-breakdown reaction. Contrib Mineral Petrol 32: 24–38

Klemme S (1998) Experimental and thermodynamic studies of upper mantle phase relations. PhD Thesis, Australian National Univ, Canberra

Klemme S, O'Neill HStC (1997) The reaction $MgCr_2O_4 + SiO_2 = Cr_2O_3 + MgSiO_3$ and the free energy of formation of magnesiochromite ($MgCr_2O_4$). Contrib Mineral Petrol 130: 59–65

Klemme S, O'Neill HStC (2000) The near-solidus transition from garnet lherzolite to spinel lherzolite. Contrib Mineral Petrol 138: 237–248

Klemme S, O'Neill HStC, Schnelle W, Gmelin E (2000) The heat capacity of $MgCr_2O_4$, $FeCr_2O_4$ and Cr_2O_3 at low temperatures and derived thermodynamic properties. Am Mineral (in press)

Lane DL, Ganguly J (1980) Al_2O_3 solubility in orthopyroxene in the system MgO–Al_2O_3–SiO_2: a re-evaluation, and mantle geotherm. J Geophys Res 85(B12): 6963–6972

Mao H, Bell P (1970) Behavior of thermocouples in the single-stage piston-cylinder apparatus. Carnegie Inst Wash Yearb 69: 207–216

Mao H, Bell P, England J (1971) Tensional errors and drift of thermocouple electromotive force in the single-stage piston-cylinder apparatus. Carnegie Inst Wash Yearb 70: 281–287

Matsui Y, Nishizawa O (1974) Iron (II)–magnesium exchange equilibrium between olivine and calcium-free pyroxene over a temperature range 800 °C–1300 °C. Bull Soc Fr Mineral Crystallogr 97: 122–130

Mattioli GS, Bishop FC (1984) Experimental determination of the chromium–aluminum mixing parameter in garnet. Geochim Cosmochim Acta 48: 1367–1371

McGlashan M (1990) The International Temperature Scale of 1990 (ITS-90). J Chem Thermodynamics 22: 653–663

Metcalfe A (1950) The use of platinum thermocouples in vacuo at high temperatures. Br J Appl Phys 1: 256–258

Mirwald PW, Getting IC, Kennedy GC (1975) Low-friction cell for piston-cylinder high-pressure apparatus. J Geophys Res 80: 1519–1525

Newton RC, Charlu RV, Kleppa OJ (1977) Thermochemistry of high pressure garnets and clinopyroxenes in the system CaO–MgO–Al_2O_3–SiO_2. Geochim Cosmochim Acta 41: 369–377

Nickel KG (1983) Petrogenesis of garnet and spinel peridotites. A study with particular reference to the role of chromium in geothermometry and geobarometry. PhD Thesis, UnivTasmania, Hobart

Nickel KG (1986) Phase equilibria in the system SiO_2–MgO–Al_2O_3–CaO–Cr_2O_3 (SMACCR) and their bearing on spinel/garnet lherzolite relationships. Neues Jahrb Mineral Abh 155: 259–287

O'Neill HStC (1981) The transition between spinel lherzolite and garnet lherzolite, and its use as a geobarometer. Contrib Mineral Petrol 77: 185–194

O'Neill HStC (1997) Kinetics of the intersite cation exchange in $MgAl_2O_4$ spinel: the influence of nonstoichiometry. Seventh Annu V.M. Goldschmidt Conf. Lunar and Planetary Inst, LPI Contrib No 921, Tucson, p 153

O'Neill HStC, Dollase WA (1994) Crystal structures and cation distributions in simple spinels from powder XRD structural refinements: $MgCr_2O_4$, $ZnCr_2O_4$, Fe_3O_4 and the temperature dependence of the cation distribution in $ZnAl_2O_4$. Phys Chem Mineral 20: 541–555

O'Neill HStC, Navrotsky A (1984) Cation distributions and thermodynamic properties of binary spinel solid solutions. Am Mineral 69: 733–753

O'Neill HStC, Palme H (1998) Composition of the silicate Earth: implications for accretion and core formation. In: Jackson I (ed) The Earth's mantle: composition, structure and evolution. Cambridge University Press, Cambridge, pp 3–126

Oka Y, Steinke P, Chatterjee ND (1984) Thermodynamic mixing properties of Mg(Al, Cr)$_2O_4$ spinel crystalline solutions at high pressures and temperatures. Contrib Mineral Petrol 87: 196–204

Perkins D, Holland TJB, Newton RC (1981) The Al_2O_3 contents of enstatite in equilibrium with garnet in the system MgO–Al_2O_3–SiO_2 at 15–40 kbar and 900–1600 °C. Contrib Mineral Petrol 78: 99–109

Pownceby MI, O'Neill HStC (1994a) Thermodynamic data from redox reactions at high temperatures. III. Activity–composition relations in Ni–Pd alloys from EMF measurements at 850–1250 K, and calibration of the NiO + Ni–Pd assemblage as a redox sensor. Contrib Mineral Petrol 116: 327–339

Pownceby MI, O'Neill HStC (1994b) Thermodynamic data from redox reactions at high temperatures. IV. Calibration of the Re–ReO_2 oxygen buffer from EMF and NiO + Ni–Pd redox sensor measurements. Contrib Mineral Petrol 118: 130–137

Presnall D, Brenner N, O'Donnell T (1973) Drift of $Pt/Pt_{10}Rh$ and $W_3Re/W_{25}Re$ thermocouples in single stage piston-cylinder apparatus. Am Mineral 58: 771–777

Roy DM, Barks RE (1972) Subsolidus phase equilibria in Al_2O_3–Cr_2O_3. Nature, Phys Sci 235: 118–119

Sen G (1985) Experimental determination of pyroxene compositions in the system CaO–MgO–Al_2O_3–SiO_2 at 900–1200 °C and 10–15 kbar using PbO and H_2O fluxes. Am Mineral 70: 678–695

von Seckendorf V, O'Neill HStC (1993) Experimental determination of the partitioning of Mg and Fe^{2+} between olivine and orthopyroxene at 900°, 1000° and 1150 °C and 1.6 GPa: constraints on activity–composition relations in binary Mg–Fe olivine and orthopyroxene solid solution. Contrib Mineral Petrol 113: 196–207

Walker B, Ewing C, Miller R (1962)Thermoelectric instability of some noble metal thermocouples at high temperatures. Rev Sci Instr 33: 1029–1040

Walter MJ, Presnall DC (1994) Melting behaviour of simplified lherzolite in the system CaO–MgO–Al_2O_3–SiO_2–Na_2O from 7 to 35 kbar. J Petrol 35: 329–359

Ware NG (1991) Combined energy-dispersive–wavelength-dispersive quantitative electron microprobe analysis. X-ray Spectr 20: 73–79

Williams D, Kennedy G (1969) Melting curve of diopside to 50 kilobars. J Geophys Res 74: 4359–4366

Witt-Eickschen G, Seck HA (1991) Solubility of Ca and Al in orthopyroxene from spinel peridotite: an improved version of an empirical geothermometer. Contrib Mineral Petrol 106: 431–439

Wood BJ (1978) The influence of Cr_2O_3 on the relationships between spinel and garnet-peridotites. In: MacKenzie WS (ed) Progress in experimental petrology. Natural Environment Research Council, Manchester, pp 78–80

Wood BJ, Banno S (1973) Garnet–orthopyroxene and orthopyroxene–clinopyroxene relationships in simple and complex systems. Contrib Mineral Petrol 42: 109–124

Wood BJ, Kleppa OJ (1984) Chromium and aluminum mixing in garnet: a thermochemical study. Geochim Cosmochim Acta 48: 1373–1375